SSW-025

Studies of Coal Oxidation Using Ion Microscopy and X-Ray Photoelectron Spectroscopy: Phase III

Final Report

OST84-00465

SSW-025

Studies of Coal Oxidation Using Ion Microscopy and X-Ray Photoelectron Spectroscopy: Phase III

Final Report

by

R.R.Martin, K.T.Aye, D.D.Johnston
and N.S.McIntyre

Surface Science Western
Faculty of Science
The University of Western Ontario
London, Ontario

Work on this project was conducted under the auspices of the
Canada Centre for Mineral and Energy Technology,
Energy Mines and Resources, Canada

DSS FILE NUMBER	:	24ST.23440-4-9284
DSS CONTRACT SERIAL NUMBER	:	OST84-00465
CANMET PROJECT NUMBER	:	
CANMET SCIENTIFIC AUTHORITY	:	Dr. J.A. McPhee

DATE: March 1987

The report should be cited as Contract Report No. OST84-00465

95pp

STUDIES OF COAL OXIDATION USING ION MICROSCOPY AND X-RAY PHOTOELECTRON SPECTROSCOPY: PHASE III

TABLE OF CONTENTS

			Page
Summary			i
Chapter 1	-	Statement of Work	1
Chapter 2	-	Introduction	4
Chapter 3	-	SIMS Imaging Studies of $^{18}O_2$ Uptake on Fusinite Coal Surfaces	7
Chapter 4	-	X-ray Photoelectron Studies of the Oxidation of Coal Surfaces	22
Chapter 5	-	Microscopic Chemical Derivatization on Coal Surfaces	33
Chapter 6	-	General Conclusions	41
		References	
		List of Figures	
		Appendix A	

SUMMARY

The oxidation of coal has been investigated using two surface-sensitive spectroscopic techniques: Secondary Ion Mass Spectrometry (SIMS) and X-ray Photoelectron Spectroscopy (XPS or ESCA). SIMS has been used to locate specific microscopic sites for oxygen fixation on a coal surface. XPS has been employed to measure sulphur and carbon chemical changes during the oxidation process.

In tracer oxygen studies, $^{18}O_2$ has been reacted with selected coal surfaces at temperatures ranging from 25°C to 110°C. SIMS analysis, carried out under high mass resolution allowed $^{18}O^+$ signals to be distinguished from those of $H_2{}^{16}O^+$. SIMS ion images of $^{18}O^+$ uptake show the strongest uptake occurs in fusinite macerals. In studies of fusinite coals, with pyrite inclusions, the oxygen uptake is shown to occur almost exclusively within the organic phase. Increased uptake occurs within areas adjacent to clay mineral inclusions in the organic phase. This constitutes evidence for clay minerals acting as a catalysts in the oxidation process. Carbon-sulphur structures are also identified within the organic area which could be important to the oxidation process.

XPS studies were conducted on selected microscopic areas of cleaved or polished coal surfaces. Oxidation at 110°C resulted in coverage of the original surface with a thin hydrocarbon layer. However, during ambient oxidation changes to specific functional groups on the surface were able to be monitored. Exposure of freshly cleaved fusinites in ambient air for a few hours results in an increase in surface oxygen contact from 10% to 15%. Oxygen fixation involves conversion of iron sulphide to various forms of oxidized sulphur.

Site specific reagents have been used in conjunction with SIMS to identify functional groups specifically involved in surface oxidation. The presence of acid groups has been sought using exchange reactions with alkaline elements such as barium. In the coals studied surface exchange during oxidation is only detected on mineral inclusions. Tollen's reagent (an ammoniacal silver solution) was used with SIMS to detect locations of carbonyl surface groups. Such groups were clearly identified in organic regions of fusinite surfaces. This approach has good potential for use in further oxidation studies.

CHAPTER 1

STATEMENT OF WORK

Ion Microscopy, a type of Secondary Ion Mass Spectrometry, is a highly sensitive analytical technique capable of detecting virtually all chemical elements in microscopically small regions. It is considered a promising approach to characterizing the complex heterogeneous structures typical of coal.

The Cameca IMA-3F Ion Microscope at Surface Science Western is being used to assess the potential of coal microanalysis using Secondary Ion Mass Spectrometry. This ion microscope (unique in Canada) allows elemental distributions in the coal to be mapped to a spatial resolution of ≈1 μm. Trace element distributions can be determined using this technique with greater sensitivity than any other known technique. Analytically difficult elements such as carbon, oxygen and hydrogen are also detectable, thus allowing both organic and inorganic phases to be characterized.

In the first phases of this work, the distributions of inorganic elements have been correlated with the maceral type in which they appear. The effects of surface oxidation of coals have also been studied using ^{18}O to distinguish reacted oxygen from that already in the coal matrix. These studies have determined oxygen uptake within individual microscopic macerals in coal specimens and have shown the higher reactivity of

fusinite toward oxidation under high temperature storage conditions (100-150°C).

In Phase III the oxidation conditions will be extended to more typical storage temperatures over a range of pressures. Other techniques will be used to complement the ion microscope studies of compositional changes in the coal.

TASKS

1. ^{18}O will be used to study the oxidation of selected macerals on polished sections of four typical Canadian coals. The oxidation conditions will be systematically varied (i.e. temperature and oxygen pressures) and rate and depth of the penetration of ^{18}O into the coal will be monitored by cross-sectioning.

2. The rates of oxidation in mineral-rich and demineralized samples of vitrinite and fusinite will be compared.

3. Coal sections sufficiently thin for infra-red spectrometry will be used to examine the nature of oxygen-containing functional groups on the coal surface. ^{18}O will be used in the oxidation, so that molecular vibration frequences observed will be well separated from these due to the background.

4. A detailed analysis of the mineral matter in coal will be undertaken by comparing specific ion intensities taken from standard mineral samples with those obtained from well-characterized macerals.

5. The chemical structure characterization of the organic matter in coal using near-static SIMS conditions will be investigated for a series of three mid-bituminous coals.

CHAPTER 2

INTRODUCTION

There has been considerable interest in the mechanisms of coal oxidation under ambient conditions (1-3). Increased oxidation lowers the energy content of the coal and alters its physical properties (4). It is very difficult to study low temperature oxidation since measurable changes occur relatively slowly. Such changes are therefore best detected at or near an interface between the coal and the oxidizing medium. In addition, coal is a very complex mixture of organic and inorganic substances, and therefore many oxidation mechanisms are possible - the relative probability of each being determined by the proximity of specific inorganic groups, organic functional groups, moisture content and the permeability of the coal. Thus it is necessary to study a collection of specimens (4) from any one type of coal in order to bracket the range of possible reactions occurring at the coal/oxidant interface.

This Report summarizes a study of low temperature coal oxidation which has involved a number of relatively new surface and microscopic analytical techniques. These techniques have been coupled with a novel experimental methodology which has yielded much new information on the chemistry of coal oxidation. Our group has prepared two earlier EMR Reports dealing with studies of the structure and oxidation of coal. One earlier Report (5) describes the first studies to use Secondary Ion Mass

Spectrometric (SIMS) images to gain an understanding of the structural relationship between organic and inorganic constituents of different coal macerals. In a second Report (6) the study of coal oxidation was initiated using SIMS. In that Report the uptake of isotopically-labelled oxygen on several characterized coal surfaces was investigated as a function of coal rank, maceral type and temperature. Among other things, it was concluded that the gas phase oxidation of fusinite macerals occurs considerably more rapidly than for other macerals, contrary to the evidence of earlier studies using chemical oxidation. It is clear that various chemical sites on the coal will react differently in different oxidation media.

The present Report focuses on aspects of coal surface chemistry which can lead to increased intake of oxygen. This has been studied using isotopically-labelled oxygen as well as specific reagent groups which react uniquely with certain chemical sites on a surface. We have used SIMS imaging for the first time to identify specific microscopic regions of the coal where reactions have occurred, and to correlate the interaction of surface regions containing different elements or functional groups.

Other chemical information has come from studies using X-ray Photoelectron Spectroscopy (XPS or ESCA). XPS chemical shifts have been used to follow the chemistry of carbon, sulphur, oxygen, iron and other elements as a function of oxidation. The

availability of high XPS spectral resolution and good spatial definition has allowed detailed assignments of the carbon and sulphur chemical species.

Finally, SIMS images have been obtained under high mass resolution conditions for the first time. Using this method we have been able to identify molecular ions with a high degree of certainty. Some of these ions appear to originate from specific functional groups on the coal surface.

The Report is divided into three chapters: ^{18}O oxidation studies, XPS oxidation studies, and chemical derivitization. The results of each study are compared in the final chapter.

CHAPTER 3

SIMS IMAGING STUDIES OF ^{18}O UPTAKE ON FUSINITE COAL SURFACES

A. Introduction

Oxygen is widely distributed in coal. Accordingly, we have elected to oxidize coal using $^{18}O_2$, thus providing an isotope tracer to identify newly oxidized regions. Secondary ion images provide accurate representations of the distribution of elements on the coal surface and are thus a powerful tool for studying the ^{18}O on the coal. This chapter presents the results obtained in a study of the ^{18}O surface distribution obtained on oxidation of selected coals and maceral types.

The information obtainable from the SIMS instrument is significantly extended by the ability to obtain both mass spectra and ion images to a mass resolution of 1:3500. High mass resolution provides sufficient additional information to make positive identification of species having the same nominal mass. For example at a nominal mass of 32 daltons, ions due to both $^{16}O_2^-$ and $^{32}S^-$ are collected. If high mass resolution is employed, the mass defect between these two species may be exploited to achieve separate ion images. These two species are only 0.018 daltons apart.

B. Experimental

SIMS studies were carried out using a CAMECA IMS 3f ion microscope which has been described in an earlier Report. (5) Previously SIMS spectra were excited using an O_2^+ or O^- primary ion beam. This work however employed a Cs^+ primary beam because it gives a better yield of electronegative elements such as oxygen and sulphur. Further, ambiguities which might be created by the presence of oxygen in the primary beam are eliminated. All results were obtained using a primary ion beam of 12 keV at 100 nA. The high mass resolving power of the IMS-3f was frequently used to distinguish more than one secondary ion species occurring at the same unit mass. For example, $^{18}O^+$ and H_2O^+ could be resolved by their mass defect differences with a mass resolution of at least M/M+1 of 800. High resolving power {M M+1)>3000} was necessary to distinguish ions at mass 40 such as C_2O^-, $C_3H_4^-$ and Ca^-. Ion images were obtained photographically as described in the previous Report. (5)

All coals studied are described in Appendix A. All except pyrite-rich fusinite were coated with 10 nm. of gold before analysis to prevent charging.

C. Results and Discussion

(i) P-587

The oxidation procedure and equipment was identical to that described in an earlier Report. (6) Oxidations were done in 0.2

atm. $^{18}O_2$, for lengths of time from 10 hours to 30 days and at temperatures between 25°C and 110°C.

Figure 1 shows a set of ion images obtained from the coal P-587 prior to its oxidation. The area displayed covers both fusinite and vitrinite regions. Figure 1(a), obtained at mass $24^-(C_2)$, serves to define the organic regions on the coal surface. The vitrinite is the featureless area. Figures 1(b) and (c) represent masses $27^+(Al^+)$ and $28^+(Si^+)$ respectively. The silicon and aluminum are confined to the fusinite region and show this area to be rich in a clay mineral, probably kaolinite. No evidence of sulphide infillings was found.

Figure 2 was obtained from a nearby area in the same coal after exposure to $^{18}O_2$ at 0.2 atmospheres pressure and 110°C for fourteen hours. Figure 2(a), the C_2^- image, identifies the organic-rich cell walls of the fusinite while 2(b), the $^{18}O^-$ image, shows that the ^{18}O uptake has occurred preferentially in the organic regions. This result is important, since the role of minerals in coal oxidation is a matter of some debate and several mechanisms have been advanced. For example, it has been suggested that clays may serve as a source of free radicals which initiate chain oxidation processes. (2) In this case, however, the results establish that significant ^{18}O uptake does not occur on the clay mineral present in this sample since it is already fully oxidized. The ^{18}O is present predominantly in the organic phase.

Figures 2(c), (d) and (e) correspond to three images all at nominal mass of 40 daltons. They are ordered in increasing fractional mass. The tentative assignments made to these species in order of increasing mass are: Ca^-, C_2O^- and C_3H_4. The C_2O^- ion is among the most prevalent heteromolecular ions detected in fusinite.

(ii) Pyrite-rich Fusinite

Figure 3 was obtained from a piece of pyrite-rich fusinite heated to 110°C in $^{18}O_2$ at 0.2 atmospheres pressure for fourteen hours. The images were obtained at masses of (a) 24^-, (b) 34^-, (c) 16^-, (d) 18^-, and (e) 56^-, respectively representing C_2^-, $^{34}S^-$, $^{16}O^-$, $^{18}O^-$ and CS^- respectively. The C_2^- and $^{34}S^-$ images define the organic and pyrite regions of the coal. Both $^{16}O^-$ and $^{18}O^-$ are found predominantly in the organic phase. The appearance of ^{18}O uniquely in this area strongly indicates that this phase is still more reactive to oxygen.

The sulphur-containing region represents the vacuoles within the prehistoric wood structure. It has been suggested that the original cell walls are coalified while the cell interior provides cavities in which a variety of water soluble minerals may be deposited. Sulfide-filled cavities such as those encountered in this specimen are thought to result from bacterial reduction of water-soluble sulfates. By contrast, groundwaters poor in sulfates deposit clay minerals which in turn weather to produce clays such as kaolinite. The coal P-587 described

earlier is representative of this latter case. It can been seen from the ^{16}O image in Figure 3 that most of the oxygen is present in the organic cell walls of the fusinite. The ^{18}O area exhibits a similar pattern to that of ^{16}O but the oxygen-rich areas are more sharply defined.

The well defined C_2S^- image is confined entirely to the organic cell walls. This suggests a chemical interaction between the organic matter and the iron sulfide within the cells. The presence of C-S bonds in these areas can be demonstrated with XPS (Chapter IV).

The same pyrite-rich fusinite was oxidized at 25°C in 0.2 atm, $^{18}O_2$. The reaction time was lengthened to 10 days in anticipation of a much slower reaction kinetics. Figure 4 shows ion images of a polished surface after the reaction. Figure 4(a), C_2^-, and 4(b), $^{34}S^-$ outline the organic and pyrite regions clearly. The $^{16}O^-$, (Figure 4(c)) and $^{18}O^-$, (Figure 4(d)) distributions clearly show that both "old" and "new" oxygen are preferentially located within the organic phase, just as was found following treatment at 110°C. The distribution of the ^{18}O in the organic phase following 25°C oxidation was also very similar to that following oxidation at 110°C. This distribution exhibited submicron variations that might suggest localized initiation of the oxidation process. Figures 4(e) and (f) are images of mass 28 and mass 30 respectively. The mass 28 image contains contributions from both $^{28}Si^-$ and $^{27}AlH^-$, while the mass

30 image has contributions from $^{30}Si^-$ and $^{12}C^{18}O^-$. Thus, the silicon distribution is unequivocally identified as those points appearing in the same location in both images. In comparing this Si distribution with the ^{18}O distribution, it is possible to see a spatial relationship between localized high concentrations of ^{18}O and the presence of silicon-containing particles. Our studies in section (i) showed that there is little uptake of ^{18}O on inorganic silicate phases. However such surfaces may catalyze the uptake of oxygen into the organic phase immediately adjacent to the silicate surface. In such cases, the tracer oxygen will appear to be closely associated with the silicate phase. This particular result is the first positive evidence of the effect of a mineral species in promoting localized oxidation of the coal.

The same area also produced some molecular ion images which suggest specific types of chemical bonding within discrete areas. In Figure 5(c) the image of $^{12}C^{16}O^-$ is shown. This was obtained under a high enough mass resolution ($M/_{MH}$ >3000) to eliminate all other secondary ions as possible contributors. The CO^- image consists of very localized pockets which do not match the general carbon or oxygen distributions in the area. Thus, we suggest that these CO^- secondary ions result from a particular molecular structure localized in certain areas of the coal. A genesis of the CO^- ion above the surface would have been expected to result in CO^- images only from areas where C_2^- and $^{16}O^-$ images coincide. The CO^- producing areas observed here are entirely in the organic region and are no larger than 1 μm diameter. Such CO^- secondary

ions could result from any moiety containing strong C-O bonds. The presence of similar $^{12}C^{18}O^-$ distribution is evident from the mass 30 image in Figure 4(f). This suggests that certain organic areas have a particularly high propensity for specific C-O addition on exposure to oxygen even at room temperature.

Figure 5 (d) also shows the distribution of the C_2S^- secondary molecular ion. It is clear from comparison with Figures 5(a) and (b) (C_2^- and C_4^- respectively) that the C_2S^- originates almost exclusively from the organic cell walls of the fusinite structure. This result is identical to that obtained from a different area of the same coal (Figure 3(e)). These observations suggest that some chemical interaction is occurring between the organic phase and the iron sulfides in the coal.

The intensities of the images for ^{16}O and ^{18}O obtained at two different temperatures in this pyrite-rich coal, can be used to estimate the activation energy for the ^{18}O uptake. The ^{16}O content of the coal should not be expected to change during oxidation with ^{18}O; thus the intensity of the ^{16}O image should be the same in coal heated to 110°C in $^{18}O_2$ as that in the coal treated in a similar fashion at 25°C. In the imaging process all instrument parameters are held constant and the exposure time used to photograph the ion images is adjusted to obtain images of approximately the same intensity. As a result the exposure time required to obtain an image is proportional to the concentration of the imaged species on the surface assuming reciprocal film

response. Figures 3(c) and 4(c) are the ^{16}O images obtained from the coal treated at 110°C and 25°C respectively. In each case the exposure time is 1/2 sec, confirming that the ^{16}O concentration has not changed.

The exposure time required to generate a satisfactory image of ^{18}O after treatment of the coal with $^{18}O_2$ at 110°C was 5 sec, Figure 3(d). A comparable image for the coal treated at 25°C required a 30 sec exposure Figure 4(d). Assuming film emulsion reciprocity, the concentration of ^{18}O on the 110°C coal is six times as great as that on the 25°C coal. This result is, of course, independent of any matrix effects or other sample parameters since the two samples are identical.

The measure of relative uptake can be converted to a ratio of rates of uptake at the two temperatures. Thus if the concentration of ^{18}O on the surface of the 25°C coal is arbitrarily assigned a value of X then the ^{18}O concentration on the 110°C coal is 6X and:

$$\text{Rate of uptake 110°C coal} = \frac{\text{concentration}}{\text{time}} = \frac{6X}{14 \text{ hrs.}}$$

$$\text{Rate of uptake 25°C coal} = \frac{X}{240 \text{ hrs.}}$$

and from the Arrhenius relationship

$$\frac{\text{Rate 110° coal}}{\text{Rate 25° coal}} = \frac{6X/14}{X/240} = 1.0 \times 10^2$$

$$= \frac{e^{-Ea/RT_{110}}}{e^{-EA/RT_{25}}}$$

$$= e^{Ea/R\left(\frac{1}{T_{25}} - \frac{1}{T_{110}}\right)}$$

where Ea = activation energy for the reaction

R = lead gas constant = 8.314 J mol^{-1} K^{-1}

T = absolute temperature

The results obtained here yield Ea = 52 kJ mol^{-1}

This result, which is independent of absolute ^{18}O concentration, is of the same order of magnitude as that expected for a catalysed free radical chain oxidation (2), assuming an O-O bond energy of approximately 100 kJ mol^{-1}. The result is in good accord with the results of Carpenter and Giddings (7) for coal oxidized under similar conditions.

(iii) P-250 COAL

Coal P-250 was also heated in $^{18}O_2$ at 0.2 atm for fourteen hours at 110°C. The results are shown in Figure 6. Figure 6(a), C_2^-, clearly defines the organic region of this coal, while Figures 6(b) and (c) show Al^+ and Si^+ within the cellular structure of a fusinite band running across the imaged field. Thus in this coal, silicate clay minerals have filled the vacancies within the cells of the fusinite. The $^{16}O^-$ image also defines the silicate region, since the clay mineral is particularly rich in oxygen. However the ^{18}O distribution is general over the organic portion of this coal surface. In the case of the fusinite band, the ^{18}O is confined largely to the cell walls (Figure 6(e)). This sample yields results in agreement with those obtained for the P-587 sample. Specifically, alumino-silicate minerals have filled voids in fusinite, and on oxidation with ^{18}O, the resulting ^{18}O image shows that the oxygen uptake is confined to the organic material.

(iv) WAYNESBURG COAL

The Waynesburg coal used in this portion of the study was supplied by the University of Western Ontario Department of Geology. It is of particular interest because it is rich in pyrites and had been used in a study of the conversion of pyrite to various iron sulfates on exposure to air. (8) In addition, it was possible to obtain large single pieces of this material and this virtually guaranteed fresh faces by sectioning large blocks.

The goal of this section of the work was to obtain a large number of mass resolved images from a section of a coal containing significant amounts of iron pyrite. Assignments of species represented by specific images should lead to some insight into the mechanism of coal oxidation. Accordingly, a piece of Waynesburg coal, was exposed to 0.2 atmospheres of $^{18}O_2$ for 33 days at 23°C. The images are divided into three categories: carbon-related, oxygen-related and sulphur-related with an arbitrary fourth category for species not readily accommodated by this scheme. Since both carbon and sulphur are frequently oxidized and there is strong evidence for C-S bonds the carbon and sulphur areas sometimes overlap. Representative images are shown in Figure 7.

Figure 7(a), (b), and (c) are the images of C_2^-, $^{16}O^-$ and $^{32}S^-$ and define the sulphur-rich and organic regions. $^{16}O^-$ is found in both the sulphur-rich and organic regions. Figure 7(d) represents the distribution of $^{18}O^-$ while 7(e) and (f) are $^{18}OH^-$ and F^- respectively. Figure 7(g) is the image obtained for $^{16}O_2^-$ while 7(h) and (i) are those of OOH^- and SH^- respectively. Figure 7(j) is the distribution obtained for C_2S^-. Thus, the collection of images in Figure 7 shows how oxygen interacts with both the carbon and sulphur in the sample. The detection of molecular ions containing ^{18}O is noteworthy since this constitutes evidence for chemical reaction between $^{18}O_2$ and the coal surface.

Since a large number of images were collected it is more convenient to display the results in tabular form. Table I lists the ions imaged, divided according to the parent element. Those cases in which the assignment is uncertain are indicated with a question mark.

The images in Figure 7 show a significant uptake of ^{18}O by the coal under very mild conditions. The molecular ions CS^- and C_2S^- are also detected in regions on or near the organic regions in the coal. This observation, coupled with the XPS detection of C-S bonds (Chapter 4) suggests that sulfonation of the coal is occurring by reaction of the organic phase with oxidation products of the pyrite, possibly sulphuric acid. Sulfonation of this type is especially interesting since the reaction is reversible. Thus, removal of the organic sulphur would be possible with mild acidification using an acid such as HCl.

TABLE 1

MASS ASSIGNMENT OF SIMS IMAGES TAKEN OF WAYNESBURG COAL AFTER OXIDATION IN $^{18}O_2$

Carbon Related Images		Sulphur Related Images		Oxygen Related Images		Other	
Mass	Assignment	Mass	Assignment	Mass	Assignment	Mass	Assignment
1^-	H^-	32^-	S^-	16^-	$^{16}O^-$	18^-	H_2O^-
12^-	C^-	33^-	SH^-	17^-	OH^-	19^-	F^-
14^-	CH_2^-	34^-	$^{34}S^-$	18^-	$^{18}O^-$	28^-	Si^-
24^-	C_2^-	34^-	$H_2{}^{32}S^-$	19^-	$^{18}OH^-$	40^-	(?)
26^-	$C_2H_2^-$	35^-	$^{34}SH^-$	32^-	O_2^-	23^+	Na^+
26^-	CN^-	36^-	$^{36}S^-$	33^-	HO_2^-	24^+	Mg^+
28^-	CO^-	44^-	CS^-	34^-	$^{16}O^{18}O^-$	27^+	Al^+
		48^-	SO^-				
36^-	C_3^-	45^-	CSH^-(?)	35^-	$H^{16}O^{18}O^-$(?)	28	Mg^+
37^-	C_3H^-	56^-	C_2S^-	37^-	$^{18}O_2H^-$(?)	40^+	Ca^+
40^-	C_2O^-	49^-	C_4H^-	48^-	O_3^-	56^+	Fe^+
40^-	$C_3H_4^-$					189^+	$CsFe^+$
42	$C_2H_2O^-$(?)						
44	CO_2^-(?)						
48^-	C_4^-						
49^-	C_4H						

(iv) CONCLUSIONS

1. Tracer oxygen uptake in several pyrite-filled fusinite coals has been studied by ion microscopy, and compared with oxygen uptake in a clay-filled fusinite. In all cases, the preferential uptake of tracer oxygen into the organic phases of the fusinite is clearly detected. While this result is not unexpected on the basis of chemical reactivity, it is viewed as proof of the SIMS technique to measure differences in reactivity on a microscopic scale.

2. The concentration of tracer oxygen in organic areas of the fusinite has been found to increase in areas containing microscopic inclusions of clay minerals. Since uptake of tracer oxygen into a mineral-only phase is not observed it is proposed that the clay mineral catalyzes the oxidation of organics at or near the clay-organic interface. This is the first direct evidence of the action of clay as a catalytic agent in coal.

3. High mass resolution has allowed a number of molecular and atomic secondary ions to be identified with much greater certainty. The distributions of two of the molecular ions, CO^- and C_2S^- suggest that they originate from molecular structures on the coal surface, and not merely from ion-molecule recombination reactions above the surface.

4. After oxidation the distribution of the C_2S^- secondary is in an area of the organic phase adjacent to pyrite-filled areas. It is proposed that sulphidation of such areas has occurred during oxidation.

5. The molecular ions $^{12}C^{16}O^-$ and $^{12}C^{18}O^-$ are detected in microscopic pockets within the organic phases of the fusinite. These ions are proposed to originate from regions of oxidized organic compounds of singularly high reactivity.

CHAPTER 4

X-RAY PHOTOELECTRON STUDIES OF THE OXIDATION OF COAL SURFACES

A. Introduction

Although there have been several recorded instances where the use of X-ray Photoelectron Spectroscopy (XPS) has been used to characterize coal (9-11) there have been few previous reports of XPS analysis of changes in a coal surface composition as a function of exposure to low temperature oxidation. XPS has several capabilities which suit such studies. Firstly, the concentration of oxygen in or on the coal surface can be monitored with a reasonable degree of quantitative reliability. Secondly the chemical states of important elements such as carbon, sulphur and oxygen can be followed during oxidation by means of the chemical shift. Finally, improvements in XPS technology have led to an ability to restrict measurements to selected microscopic regions. Thus, XPS measurements can frequently be confined to a specific maceral or to a region of a maceral which can be identified optically with a feature such as mineralization.

XPS oxidation studies were conducted on three specimens: P-587, P-250 and the special pyrite-rich fusinite. The P-587 and P-250 surfaces were polished and subjected to petrographic analysis. The specialty fusinite coal, by contrast, was fractured immediately before analysis. Specimens P-587 and P-250

were oxidized at 110°C in air for 48 hours, while the pyrite fusinite was exposed to ambient air for 60 hours. In each case, care was taken to reanalyze the same area of the specimen surface.

Photoelectron spectra were taken on a customized system designed around a Surface Science Laboratories SSX-100 spectrometer. The exciting Al Kα radiation is monochromatized, so that the photoelectron linewidths are 0.5 - 0.8 eV narrower than in a conventional spectrometer. This was particularly important for resolution of the C(1s) and S(2p) spectra which frequently consisted of peaks from multiple chemical states. Spectra were usually taken from regions as small as 150 μm diameter (effectively on ellipse with major and minor axes of 200 and 110 μm).

The energy scale of the spectrometer was calibrated using an $Au4f_2$ binding energy of 83.90 eV. Coal surfaces usually exhibited charging and this was compensated using an electron flood gun. In such cases it was necessary to provide a secondary calibration binding energy from species present on the surface. In the case of the pyrite coals, the $Fe2p3_{/2}$ line for FeS_2 was used (B.E. = 706.9 eV). In other cases the hydrocarbon C(1s) line (B.E.-284.9 eV) was used, but this was often compromised by the complex C(1s) lineshape due to multiple chemical states.

B. Results

(i) P-587

The features on the section of P-587 coal used in this study are shown in the optical micrograph in Figure 8. Three areas were chosen for XPS analysis, and these are circled in the Figure. Area 1 was a featureless area of vitrinite. Area 2 contained visible mineralized areas, but was still in the vitrinite. Area 3 was in a fusinite maceral.

Broad range spectra of Areas 1, 2 and 3 are compared in Figures 9 (a-c). For each spectrum, the elemental compositions are shown determined from peak intensities corrected for photoelectron cross-section. The composition of both vitrinite areas (Figures 9 a and b) is fairly similar with only a minor increase in silicon in the area with the mineralized appearance. The oxygen content of 5-6% is attributable mainly to organically-bonded oxygen, in the absence of significant inorganic species. The fusinite area (Figure 9 (c) is seen to have a higher oxygen concentration as well as detectable higher concentration of sodium, aluminum and silicon. The nitrogen concentration is seen to be similar in all areas. Of particular note is the concentration of nitrogen in two of the areas. C(1s) lineshapes determined for Area 1 and Area 3 are compared in Figure 10. The major carbon species detected in Area 1 (Figure 10(a)) are identified as "amorphous" carbon and hydrocarbon. A minor component due to C-O bonding is detected. In order to account for the total concentration of oxygen (6%) the C-O bonds must

represent bridging oxygens attached to 2 carbons. In the fusinite area however some evidence of C-OH and C-OH = O bonding is seen in the C(1s) spectrum (Figure 10(b)).

Following oxidation in air at 110°C for 48 hours the same areas of P-587 were reanalyzed. Figure 11 shows spectra of Area 3 (fusinite) following oxidation. Surprisingly, the surface oxygen concentration has decreased, but this is due to an increase of hydrocarbon on the surface. The C(1s) spectrum in Figure 11(b) exhibits almost no C-O bonding compared to the spectrum (Figure 10(b)) found before the oxidation. It appears that heating of coal specimens during oxidation leads to coverage of the surface by a very thin hydrocarbon film, presumably by diffusion from the interior. However silica is still detected on the surface (Figure 11(a)) and this suggests that the inorganic phase is not covered with hydrocarbon.

C. P-250

Two areas of a polished section of P-250 coal were analyzed. No photographic record was kept since the areas did not have any particular microscopic features which might characterize one from another. A spectrum of one of the areas is shown in Figure 12(a). The other area was less mineralized. The P-250 coal has a considerably higher oxygen content than P-587, even allowing for the greater number of inorganic oxides. The nitrogen content is also very high. The bonding of oxygen and nitrogen to carbon can be confirmed by the fitted C(1s) spectrum shown in Figure

12(b). In this spectrum, some of the peaks fitted under the envelope are assignable; the position of the peak (#5) at a corrected B.E. = 288.4 eV suggests an aldehydic structure, while the peak (#4) around 287.2 eV is assignable to a number of possible C-O and C-N single bond linkages. Similar carbon structures were observed in the other sample area. Evidence of a conjugated structure is obtained from the presence of a weak shake-up peak in Figure 12(b) (#6). The position of this peak correlates to peak 4 which suggests a heterocyclic aromatic ring structure is a significant component of the organic phase. Analysis of the same area after oxidation for 48 hours at 110°C gives the spectrum shown in figure 12(c). In this spectrum it appears that the nitrogen and oxygen concentration have dropped to one third of their former values. Again, this could be due to a surface coverage by a light non oxygen-bearing hydrocarbon which could have diffused from the bulk during heating. As in P-587 the silicon concentration remains high on the surface after heating, while all other species, except hydrocarbon decrease.

D. Pyrite Fusinite

This coal was known to have a high sulphur concentration with much of the sulphur contained in cells (see Figure 3). Therefore polishing was not attempted since preferential removal of the most sulphur-rich phase was likely. A number of cleavage surfaces were analyzed all showing roughly similar total sulphur concentrations but exhibiting considerable variation in the chemistry of the sulphur, as well as in the other elements

present. The group of spectra shown in Figure 13 show one typical area (Area A) on a freshly cleaved surface. The total spectrum (see Figure 13(a)) shows that sulphur species comprise about 11% of the sulphur, while the oxygen concentration at 13% is typical of other fusinites analyzed. Only one form of iron is recognized in the detailed Fe(2p) spectrum in Figure 13(b) the sharp Fe($2p^3/_2$) peak at 707 eV is typical of iron pyrite, FeS_2 (12). The detailed S(2p) spectrum shown in Figure 13(c) can be mathematically resolved into contributions from four major chemical species (each species produces a spin-orbit-split doublet). The S($2p^3/_2$) peak (#1) with the lowest binding energy (charge-corrected B.E. = 162.4 ± 0.2 eV) is clearly assignable to sulphur bonded as inorganic FeS_2 (12) while peak #2 that at B.E. = 163.4 eV± O.2 eV is ascribed to sulphur bonded as an organic sulphide (13). Elemental sulphur, another possible species is eliminated since its binding energy is about 0.5 eV higher. The two sulphur species at higher binding energies are assigned as oxidized sulphur compounds. The S($2P^3/_2$) peak at B.E. = 168.3 eV (#3) is assigned to sulphur bonded as an organic sulphonate (C-S-O) (13c) while that at B.E. = 169.1 eV (#4) is assigned to inorganic $FeSO_4$. Based on the total oxygen measured on the surface (13%), and the quantity of sulphur-oxygen bonds, it is calculated that there is 8% oxygen bonded directly to carbon. Figure 13(d) shows the C(1s) spectrum for this surface. The major peak (#1) is due to hydrocarbon, while the second prominent

respectively. Thus, both Figures 13(c) and 13(d) present evidence for the C-S bonding in a coal containing pyrite.

The Fe(2p), S(2p) and C(1s) spectra for another freshly cleaved surface (specimen B) are shown in Figure 14. The Fe(2p) spectrum (Figure 14(a)) can be resolved into a low B.E. FeS_2 component (#1) and a higher B.E. component (#2), which could be due to FeS (phyrrotite) and/or iron oxides. The S(2p) spectrum (Figure 14(b)) helps to clarify this. In addition to the sulphide bonded as FeS_2 and C-S on this surface an additional $S(2p^3/_2)$ peak at B.E. = 161.6 ±.2 eV can be assigned to sulphur bonded as FeS (12). The concentration of S-O bonds on this surface is seen to be less than for specimen A. However, the total oxygen concentration for this area was measured to be 12%. Much of the oxygen is directly bonded to carbon. The C(1s) spectrum showing the oxidized carbon is seen in Figure 14(c). The fitted spectrum shows the presence of carboxyl, aldehydic and ether oxygen linkages in addition to the major peaks due to amorphous carbon and hydrocarbon.

Pyrite fusinite cleaved along the cell structure (longitudinally) rather than across the structure (transverse) gave a surface composition with more iron, more sulphur and more oxygen (see Figure 15). This specimen (specimen C) was oxidized by heating in air at 70°C for a period of 15 hours. It was hoped that, at this lower temperature, less hydrocarbon migration to the surface would result and the course of the oxidation could be

clearly followed by XPS. Figure 16(a) shows the total spectrum of the same region after oxidation. The sulphur concentration has not changed significantly, but there has been a redistribution in its chemical forms as seen from the S(2p) spectra in Figure 16(b) The concentration of oxidized sulphur species has increased, and the amount of organic sulphide bonding has decreased. The C(1s) spectrum in Figure 16(c) shows little evidence of C-O bonding and it appears that the number of C-O bonds has decreased with heating. On the basis of this information it appears that oxygen in the coal is preferentially bonded to sulphur after mild heating.

Oxidation at room temperature using longer exposures was also studied. Spectra of a freshly-cleaved transverse-orientation are shown in Figure 17 prior to long air exposure. Figure 17(a) shows the specimen to have a high amount of oxide even before the oxidation. Much of this is present as oxidized organic sulphur compounds. The S(2p) spectrum in Figure 17(b) shows that a variety of oxygen-sulphur bonds exist in compounds other than iron sulphate (peak #3 in 17(b)(ii)). After 60 hours exposure to room temperature air, the same spot on the specimen was reanalyzed, and these are shown in Figures 17(c) and (d). The broad spectrum in Figure 17(c) shows that the total oxygen concentration has increased from 34 to 38%, compared to Figure 17(a). From the Fe(2p) line shape, the quantity of FeS_2 is seen to have decreased in favour of some oxidized form of iron, either a sulphate or an oxide. The S(2p) spectrum in Figure 17(d) shows

more detail of the oxidized sulphur species. It shows major peaks due to both iron sulphate (peak 3) and C-S-O bonding (peak 2).

These room temperature results confirm that the oxidation of FeS_2 in pyrite coals is the primary mechanism of attaching oxygen. Some oxygen is bonded as iron sulphate, some probably as iron oxides and some as an organic-sulphur oxygen compound. Unfortunately the carbon C(1s) spectra were not clear enough to quantify the amount of carbon involved in these reactions.

E. Discussion

X-ray photoelectron spectra of the coal specimens have revealed new chemical bonding information on surface oxidation processes, and as well, has provided accurate quantitative elemental analysis of surface areas as small as 300 microns in diameter. In P-587 the oxide concentration is about 5% with vitrinite macerals and somewhat higher in the fusinite maceral. Based on the small concentration of mineral matter present, it appears that most oxygen is organically bonded. The C(1s) spectrum shows most oxygen is singly bonded, in bridging fashion between two carbons. In the fusinite macerals of P-587 a greater range of oxygen bonding structures is found, including carboxyl, carbonyl and hydroxyl forms.

In the pyrite fusinite the oxygen content is higher than any maceral in P-587. Some of it is directly bonded to organic sulphur and some is bonded to carbon or iron.

Oxidation of any of the coals at 110°C results in a decrease, not an increase in oxygen. During the heating the original surface is covered by a light hydrocarbon film, which presumably diffuses from the bulk and masks any evidence of oxidation. If the oxidation temperature used is much lower than 110°C, surface compositional changes should occur at a very slow rate. However, in the case of the pyrite fusinite coal, changes in oxygen content and chemical bonding could definitely be observed after oxidation, even at temperatures as low as 25°C. Oxygen fixation on pyrite-containing coals clearly appears to occur through oxidation of sulphide groups, both iron sulphide (FeS_2) and organically-bound sulphur. The products are iron sulphates and organic species containing sulphur-oxygen groups.

There is clearly much more to do to study these and later chemical changes on the coal surfaces. The use of labelled oxygen (^{18}O) and surface vibrational spectroscopies appear attractive for use in following the reaction progress. Laser Raman studies will be instigated in the next contract to achieve a better understanding of the relationship between surface composition, time, temperature and oxygen pressure.

F. Conclusions

(1) The quantity and chemistry of oxygen on a number of different maceral surfaces has been analyzed for coal P-587. Fusinite macerals contain ≈10% oxygen, while in the vitrinite the oxygen concentration is 5%.

(2) Coal P-250, a fusinite coal, has an oxygen concentration of 14% and evidence of much carbonyl and hydroxyl bonding. Nitrogen concentration is also high.

(3) Pyrite fusinite coals contain much C-S bonding, as well as iron-sulphur bonds. Oxidized sulphur is detected, both as iron sulphate and as several carbon-sulphur-oxygen species.

(4) Oxidation of all coals at 110°C results in a coverage of the surface with a thin hydrocarbon film.

(5) Oxidation of pyrite fusinite coal shows that oxygen fixation occurs through the C-S bond.

CHAPTER 5

MICROSCOPIC CHEMICAL DERIVITIZATION ON COAL SURFACES

A. Introduction

It is possible to carry out specific reactions on coal surfaces and to use the results as a probe of the coal's chemistry. A good example of such work is provided by Painter and coworkers (14) who reacted coal with $Ba(OH)_2$ to obtain a measure of the acidic OH concentration in the coal, both by measuring the Ba uptake and using FTIR to monitor simultaneous changes in the O-H vibrational frequency. We have sought to extend the use of such site-specific reagents and to correlate the surface distribution of reaction products, as measured by SIMS, with the distribution of functional groups on the coal surface.

B. Experimental

The experimental regime was designed to test novel derivalization reactions of increasing complexity on the coal surface. In the first sequence a fresh surface of the coal P-587 was exposed to 0.01 M KOH for one hour, the resulting surface was washed briefly and the distribution of potassium on the coal surface was monitored using both SIMS and Scanning Electron Microscopy.

The results permitted both an estimate of potassium uptake by the coal and a comparison of the relative efficiency of the two

techniques. Two other fresh coal surfaces were examined using SIMS. The first was that of a fresh sample of P-302 treated for one hour with .01M KOH, the second was fresh P-251 treated for an hour with 0.01M $Ba(OH)_2$.

Tollen's reagent ($AgNO_3$ in saturated ammonia igueous solution) was also was also tested on a coal surface. The Ag^+ is reduced to Ag metal by aldehydes. A section of pyrite-rich fusinite was heated in air to 150°C for twenty-four hours, then reacted with Tollen's reagent. SIMS was used to monitor the Ag deposited on the coal surface as a result of reduction of Ag^+ by aldehydes or other easily oxidized functional groups. Relatively severe conditions were selected to help insure positive results.

When the results from the heated pyrite-rich coal proved to be positive a second piece of the same material, without prior oxidation, was treated with Tollen's reagent followed by exposure to .01M $Ba(OH)_2$ for 10 minutes. SIMS was then used to map the surface distributions of Ag and Ba on the assumption that barium carboxylates would be expected to form at sites where silver had deposited as a result of oxidation of aldehydes or related functional groups.

Finally a sample of coal P-587 was heated to 150°C for 24 hours in 0.2 atm $^{18}O_2$, followed by treatment with Tollen's reagent and exposure to 0.01M KOH for 10 minutes.

SIMS analysis was carried out on the surface in the expectation that new sites of oxidation would be revealed by the ^{18}O distribution, readily oxidized functional groups would be associated with Ag the distribution and K carboxylates would identify acidic hydrogens.

C. Results and Discussion

(i) Coals Reacted with Base only

Figure 18 shows a comparison of the results obtained with SEM and SIMS from the piece of P-587 coal without prior oxidation soaked in 0.01 M KOH for one hour. Figure 18(a) is a SEM photograph of the boundary between a fusinite and a vitrinite maceral while Figure 18(b) shows the distribution of K as measured by an X-ray fluorescence map of the same surface. This distribution is quite uniform. However, SEM/EDX samples to a depth of several thousands of angstroms thus producing a result which is not an accurate representation of the surface distribution of the K. Figure 18(d) is a SIMS step scan of the same region. It is clear that the surface concentration of the K increases by two orders of magnitude on entering the mineralized region of the fusinite maceral. This result is entirely in agreement with that expected for a cation exchange reaction between the KOH solution and the alumina silicate material previously identified within the fusinite macerals of this coal.

Figures 19 and 20 present images obtained from fresh sample of P-302 and P-251 coals, the first treated with 0.01 M KOH the

second with 0.01 M $Ba(OH)_2$. Figures 19(a), (b), (c) and (d) are those of the C_2^-, Si^+, Al^+ and K^+ ions respectively. The C_2^- image, obtained within a band of homogeneous vitrinite is bisected by an aluminosilicate phase identified both by gaps in the C_2^- image and by the distribution of Si^+ and Al^+ ions. The accompanying K^+ image indicates that, as with the P-587 sample the dominant sources of K^+ ions are the mineral phases. This is certainly due to ion exchange between the mineral matter and the KOH solution, though some suggestion remains that potassium carbonxylates may be formed close to the inorganic material.

Figures 20(a), (b) and (c) the images obtained for C_2^-, Na^+ and Ba^+, and represent results identical to those obtained for the KOH treatment of P-302, in this case the region chosen in P-251 is a homogeneous vitrinite with indwelling mineral matter, identified in this case by the Na^+ image. Essentially all the reaction product resulting from treatment with $Ba(OH)_2$ is barium cation exchange with the mineral matter.

The net result of this portion of the work, reaction of fresh, high rank coal with base, is the conclusion that if carboxylates are formed at all, as is unlikely in any case, they are not detected in any definitive way in this study. There is, however, considerable well defined cation exchange between aluminosilicate mineral matter in the coal and the cations of the base.

(ii) Tollen's Reagent

Figure 21 presents the images obtained from the pyrite-rich fusinite after being heated to 150°C in air for 24 hours, then treated with Tollen's reagent. It represents our first attempt to prepare novel derivatives which could be readily correlated with organic functional groups which result in products readily identified by SIMS. Figure 21(a) shows the distribution of C_2^- and hence the organic areas on the resulting surface. Figure 2(b) shows the Fe^+ distribution which differs considerably from the organic phase. Figure 2(c), $^{16}O^+$, shows that most oxygen is associated with the organic material, while the coincidence of the silver image, 21(d), with those of both C_2^- and $^{16}O^-$ is most striking. We conclude that the deposition of silver on the coal surface is due to reaction of the silver ion with oxygen functional groups such as aldehydes. Any reaction between Fe^{2+} and Ag^+ to yield Fe^{3+} and Ag can be ruled out because there is no significant coincidence between the Fe^+ and Ag^- secondary ion images.

These very encouraging results led us to use Tollen's reagent to investigate pyrite-rich fusinite which had not been pre-treated in any way and to add the refinement of reacting the surface obtained from the Tollen's test with $Ba(OH)_2$. Figure 22 shows the results of a SIMS study of the product surface. Figure 22(a) and (b), C^- and C_2^- once again define the organic regions while 22(c), O^-, shows the material to be heavily oxidized. The Ag^- distribution is in excellent agreement with that of C_2^- and

Ba^-. It is clear that regions rich in Ag are also rich in Ba and therefore almost certainly indicate areas where reduction of silver ion has resulted in the production of carboxylic acids which subsequently react with base to produce barium carboxylates.

Figure 23 presents a sequence of reaction products identified by SIMS after treatment of the coal P-587 by first heating in $^{18}O_2$ followed in turn by reaction with Tollen's reagent and KOH. Figure 23(a), C^-, shows a rich organic phase with voids indicating bands of apparently detrital mineral matter associated with the coal bedding. Figure 23(b), Si^-, confirms the distribution of an aluminosilicate mineral phase within the coal. Figure 23(c), that of $^{18}O^-$ shows, as noted previously in this study, that uptake of ^{18}O by the mineral matter is not significant relative to its uptake by the organic phase of the coal. Figure 23(d), Ag^-, shows Ag deposition in well defined striations probably indicative of the direction of the coal bedding and, in most cases, closely associated with the regions immediately adjacent to clay minerals. This constitutes further direct evidence for catalytic activity by the mineral matter. Finally the K image, Figure 33(b) is clearly intimately related to the silver image, once again the result of carboxylate formation, however, the mineral matter, especially the void space due to a large mineral inclusion in the lower half of the image is less well defined. This is undoubtedly the result of K cation exchange with the mineral matter. There is no evidence that Ag

deposits on the minerals, thus the Ag image, combined with that of ^{18}O shows that oxidation resulting in aldehydes or closely related functional groups occurs in well defined regions which appear to be the result of catalytic action by aluminosilicate minerals.

D. CONCLUSIONS

1. Fresh high-ranked coals treated with KOH or $Ba(OH)_2$ did not show evidence for carboxylate formation. Only cation exchange with the mineral phase was observed.

2. Tollen's Reagent reacted readily with oxidized coals to reveal specific sites in the organic region which preferentially absorb the reagent. These sites are believed related to high concentrations of carbonyl groups.

CHAPTER 6

GENERAL CONCLUSIONS

This work has made some advances in understanding the oxidation of coal. These are listed below.

1. We have shown that in coals containing fusinite, oxygen appears to be present in higher concentration within the fusinite than within the surrounding coal areas. Also, the ^{18}O uptake on mild oxidation is more pronounced in fusinite than in any other maceral.

2. ^{18}O uptake by aluminosilicate minerals in coal is not an important process.

3. It is sometimes possible to relate images of oxygen-containing molecular ions to the presence of oxygen functional groups on the coal surface.

4. Tracer oxygen uptake within the organic phase of coal can often be related directly to the presence of aluminosilicate minerals. This provides direct evidence for catalytic activity.

5. Coal organic matter immediately adjacent to iron sulfides and sulfates serves as a rich local source of the molecular

ions C_2S^- and CS^-. XPS of these regions shows C-S bonds to be present. This implies an intimate chemical interaction between the two species.

6. Fresh, high ranked coals treated with base did not show evidence for carboxylate formation, the only significant process observed in these cases was cation exchange with clay minerals.

7. Tollen's reagent reacted readily with coals heated to 150°C in air and/or $^{18}O_2$ and with some untreated coals (but not P-302 or P-251) to produce unique Ag images associated with oxidized organic regions on the coal.

8. Reaction of coal with $^{18}O_2$, Tollen's reagent and strong base lead to selective oxidation of the coal surface with strong evidence for catalytic activity by clays.

9. Ion images may be used to obtain a crude estimate of the activation energy for the oxidation process in coal. The value of 51 kJ mol^{-1} obtained is not inconsistent with a catalyzed free-radical oxidation process.

10. From XPS studies, the oxidation of coals at temperatures of ≈ 100°C is shown to lead to the growth of a thin hydrocarbon layer on the coal surface. This is not observed at during ambient oxidation.

11. Ambient oxidation of pyrite-rich coals results in uptake of oxygen by the sulphur group.

Taken together, these conclusions support two suggested mechanisms for coal oxidation. The first, free radical chain oxidation is consistent with the presence of aldehydes implied both by sources of CO^- and reaction with Tollen's request. These would be the products of chain terminating steps. In addition we have observed relatively high concentrations in regions adjacent to small clay inclusions, which would be the result of catalytic activity by clays, as expected for a free radical mechanism. As well a rough estimate of the activation energy of the oxidation process is available from ^{16}O and ^{18}O image intensities. The result of ≈51 kJ while subject to considerable error is in surprisingly good agreement with that expected for a catalysed free radical mechanism.

The second mechanism may well be complementary to the first. It has been suggested that self-heating of coals can result from oxidation of pyrite followed by the formation of hydrated iron sulfates and sulfuric acid. These reactions, and the heat of solution of sulfuric acid are all highly exothermic and thus facilitate oxidation. Images of the molecular ion C_2S^- have been found to be intimately associated with the coal organic phase closest to pyrite inclusion. Further, XPS data confirms the presence of C-S bonds in these regions and identifies

sulphonation as a major reaction during oxidation. We suggest that sulfonation of coal takes place readily during the oxidation of pyrite because of the local concentration of sulfuric acid. If this mechanism is operative then the coal should be easily desulfured with mild HCl since sulfonation is a reversible reaction.

REFERENCES

1. Ignasiak, B.S., Nandi, B.N., and Montgomery, D.S., "Oxidation Studies on colking Coal related to Weathering: I Chromatographic Analysis of Pyrolysis Gases as a Method for Studyhing Coal Weathering", Fuel, 1970. 49, 214-221.

2. Cole, D.A., Herman, R.G., Simmons, G.W., and Klier, K., "Generation of Free Radicals in Partial Oxidation of Coal", Fuel, 1985, 64, 303-306.

3. Martin, R.R., McIntyre, N.S., Winder, C.G., Saunders, D.C., Johnston, D.D. and MacPhee, J.A., "Detection of Low Temperature Oxidation of Coal on a Microscopic Scale using Secondary Ion Mass Spectroscopy," Fuel, 1986, 65, 1313-1316.

4. Wachowska, H.M., Nandi, B.N. and Montgomery, D.S. "Oxidation Studies on Coking Coal related to Weathering: IV Oxygen Linkages influencing the Dilatomic Properties and the Effect of Cleavage on Ether Linkages", Fuel, 1974, 53, 212-219.

5. McIntyre, N.S., Chauvin, W.J. and Martin, R.R. "Characterization of Coal Surfaces by Ion Microscopy, Phase 1: Analysis of Coal Microstructure". Contract Report No. OSU-00327 for the Canada Centre of Mineral and Energy Technology, Energy Mines and Resources Canada (1983).

6. Martin, R.R. and McIntyre, N.S. "Characterization of Coal Surfaces by Ion Microscopy, Phase II: Surface Oxidation", Contract Report No. OST-00145 for the Canada Centre of Mineral and Energy Technology, Energy Mines and Resources, Canada (1985).

7. Carpenter, D.L. and Giddings, D.G., "The Initial Stages of the Oxidation of Coal with Molecular Oxygen, I-Effect of Time, Temperature and Coal Rank on the Rate of Oxygen Consumption", Fuel, 1964, 45, 247-266.

8. Wiesse, R.G., Powell, M.A. and Fyfe, W.S., "Spontaneous Formation of Hydrated Iron Sulphates on Laboratory Samples of Pyrite- and Marcasite-Bearing Coals," Chemical Geology - in print.

9. Dutta, S.N., Dowerah, D. and Frost, D.C., "Study of Sulphur in Assam Coals by X-ray Photoelectron Spectroscopy," Fuel, 1983, 62, 840-841.

10. Perry, D.L. and Grint, A., "Application of XPS to Coal Characterization" Fuel, 1983, 62, 1024-1033.

11. Clark, D.T. and Wilson, R., "ESCA Applied to Aspects of Coal Surface Chemistry", Fuel, 1983, 62, 1034-1040.

12. Binder, H.Z. fur Naturforsch, 1973, B28-5, 256-260.

13. Lindberg, B.J., Hamrin, K., Johonsson, G., Gelius, U., Fahlmann, A., Nordling, C. and Siegbahn, K., Phys. Scripta, 1970, 1, 277-290.

14. Starsinic, M., Otake, Y., Walker, P.L. and Painter, P.C., "Application of FTIR Spectroscopy to the Determination of -COOH Groups in Coal," Fuel, 1984, 63, 1002-1007.

LIST OF FIGURES

Figure 1: Ion images of coal P-587 showing the boundary between fusinite and vitrinite with alumino-silicate in the fusinite. The field displayed is 400 μm.

Figure 2: Ion images of coal P-587 after oxidation in $^{18}O_2$ for 14 hours at 110°C showing C_2^-, $^{18}O^-$, Ca^-, C_2O^- and $C_3H_4^-$. The field displayed is 170 μm.

Figure 3: Ion images of pyrite-rich fusinite oxidized in $^{18}O_2$ for 14 hours at 110°C showing C_2^-, $^{34}S^-$, $^{16}O^-$, $^{18}O^-$ and C_2S^-. The field is 170 μm.

Figure 4: Ion images of pyrite-rich fusinite oxidized in $^{18}O_2$ for 10 days at 25°C showing C_2^-, $^{34}S^-$, $^{16}O^-$, $^{18}O^-$, $^{28}Si^-/AlH^-$, $^{30}Si^-/C^{18}O^-$.

Figure 5: Another area of the pyrite-rich fusinite in Figure 4 expanded to show C_4^-, CO^- and C5 illustrating local sources of CO^- and C-S molecular ions.

Figure 6: Ion images of coal P-250 showing negligible ^{18}O uptake on clay inclusion in fusinite.

Figure 7: Ion images of Waynesburg coal showing a suite of molecular ions indicative of sulfonation and free radical oxidation.

Figure 8: Optical micrograph of a polished section of P-587 surface. The three areas (a-c) analyzed by XPS are defined by the white circles.

Figure 9: XPS total elemental scans of the three areas on a P-587 surface designated in Figure 8. (a) vitrinite (no features) (b) vitrinite (mineralization) (c) fusinite.

Figure 10: XPS detailed carbon C(1s) spectra of vitrinite and fusinite surfaces in (a) + (c) of Figure 9.

Figure 11: XPS spectra of the surface of a fusinite maceral within P-587 after oxidation at 110°C for 48 hours (a) total elemental scan (b) carbon C(1s) line.

Figure 12: XPS spectra of a selected area of coal P-250 before and after oxidation (a) total elemental scan before oxidation (b) C(1s) line before oxidation (c) total elemental scan after oxidation (d) C(1s) line after oxidation.

Figure 13: XPS spectra of a transverse freshly-cleaved surface of a pyrite fusinite coal (Area A) (a) total elevated (b) Fe(2p) line (c) S(2p) line.

Figure 14: XPS spectra of a second transverse freshly-cleaved surface of a pyrite fusinite coal (Area B) (a) total elemental spectrum (b) S(2p) line (c) C(1s) line.

Figure 15: XPS spectra of a freshly-cleaved longitudinally-oriented surface of a pyrite fusinite coal before oxidation (Area C) (a) total elemental scan before oxidation (b) S(2p) line (c) C(1s) line.

Figure 16: XPS spectra of Area C after air oxidation at 70°C for 15 hours. (a) total elemental scan (b) S(2p) line (c) C(1s) line.

Figure 17: XPS spectra of a freshly-cleaved transversely-oriented surface of a pyrite fusinite coal (Area D) before and after air oxidation at 25°C for 60 hours. (a) total elemental scan before oxidation (b) S(2p) line before oxidation (c) total elemental scan after oxidation (d) S(2p) line after oxidation.

Figure 18: (a) SEM photograph of vitrinite/fusinite boundary in coal P-587.
(b) EDX dot map of Si distribution across the boundary.
(c) EDX dot map of K distribution across the boundary.
(d) SIMS step scan for K and Al across the vitrinite/fusinite boundary.

Figure 19: Ion images obtained from P-302 treated with KOH.

Figure 20: Ion images obtained from P-251 treated with $Ba(OH)_2$.

Figure 21: Ion images obtained from pyrite-rich fusinite, heated in air and treated with Tollen's reagent.

Figure 22: Ion images obtained from pyrite-rich fusinite, treated with Tollen's reagent followed by $Ba(OH)_2$.

Figure 23: Ion images obtained from P-587 heated in $^{18}O_2$ followed by treatment with Tollen's reagent and KOH.

APPENDIX A

DESCRIPTIONS OF COAL USED IN PHASE III STUDIES

COAL	MOISTURE	ASH	VOLATILE MATTER	ELEMENTAL COMPOSITION %			
				C	H	N	S
P-302	0.78	2.37	34.26	84.3	5.3	2.1	0.7
P-250	1.12	1.33	32.6	84.0	5.8	1.8	0.5
P-251	1.12	1.33	32.6	84.0	5.8	1.8	0.5
P-587	0.29	9.61	18.15	80.8	4.1	1.2	0.3
Pommer	0.74	26.86	16.31	52.17	1.60	0.40	19.90
Waynesburg	2.0	18.7	34.1	63.4	4.7	1.1	2.1

+ Pyrite Rich Fusinite
+ Waynesburg

A
B
C
C_2^-
1/8 s
Al^+
1s
Si^+
2s

Fig.1

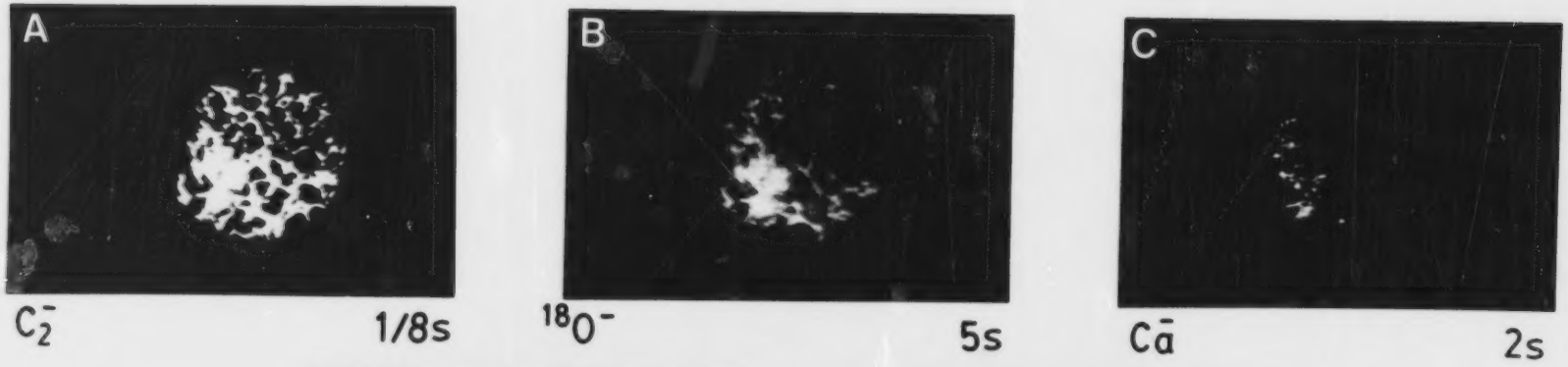
A
B
C
C_2^-
1/8s
$^{18}O^-$
5s
$C\bar{a}$
2s

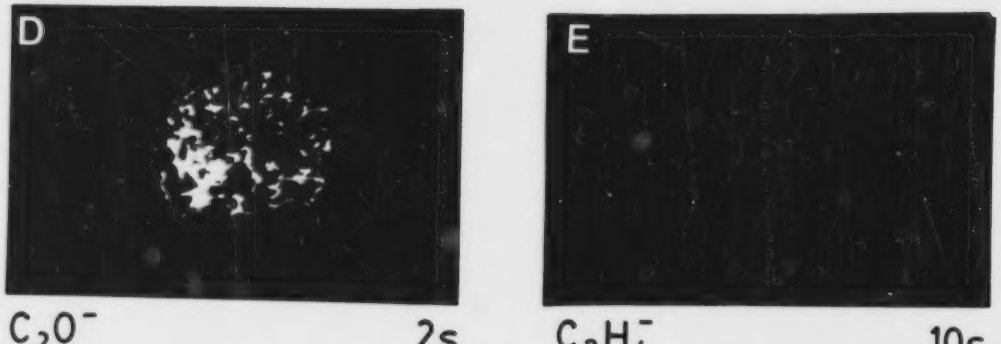
D
E
C_2O^-
2s
$C_3H_4^-$
10s

Fig. 2

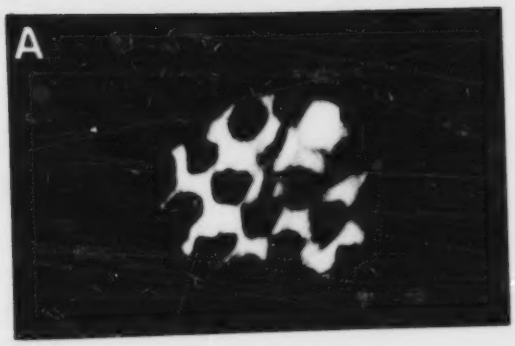

C_2^- 1/4s

$^{34}S^-$ 1s

$^{16}O^-$ 1/2 s

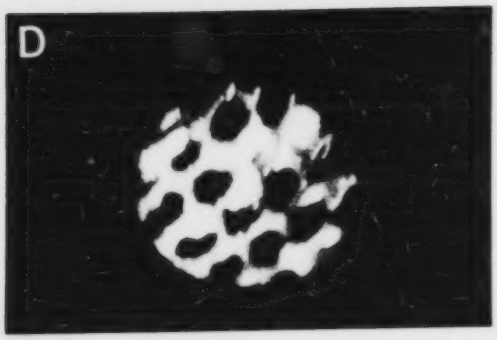

$^{18}O^-$ 5s

C_2S^- 60s

Fig. 3

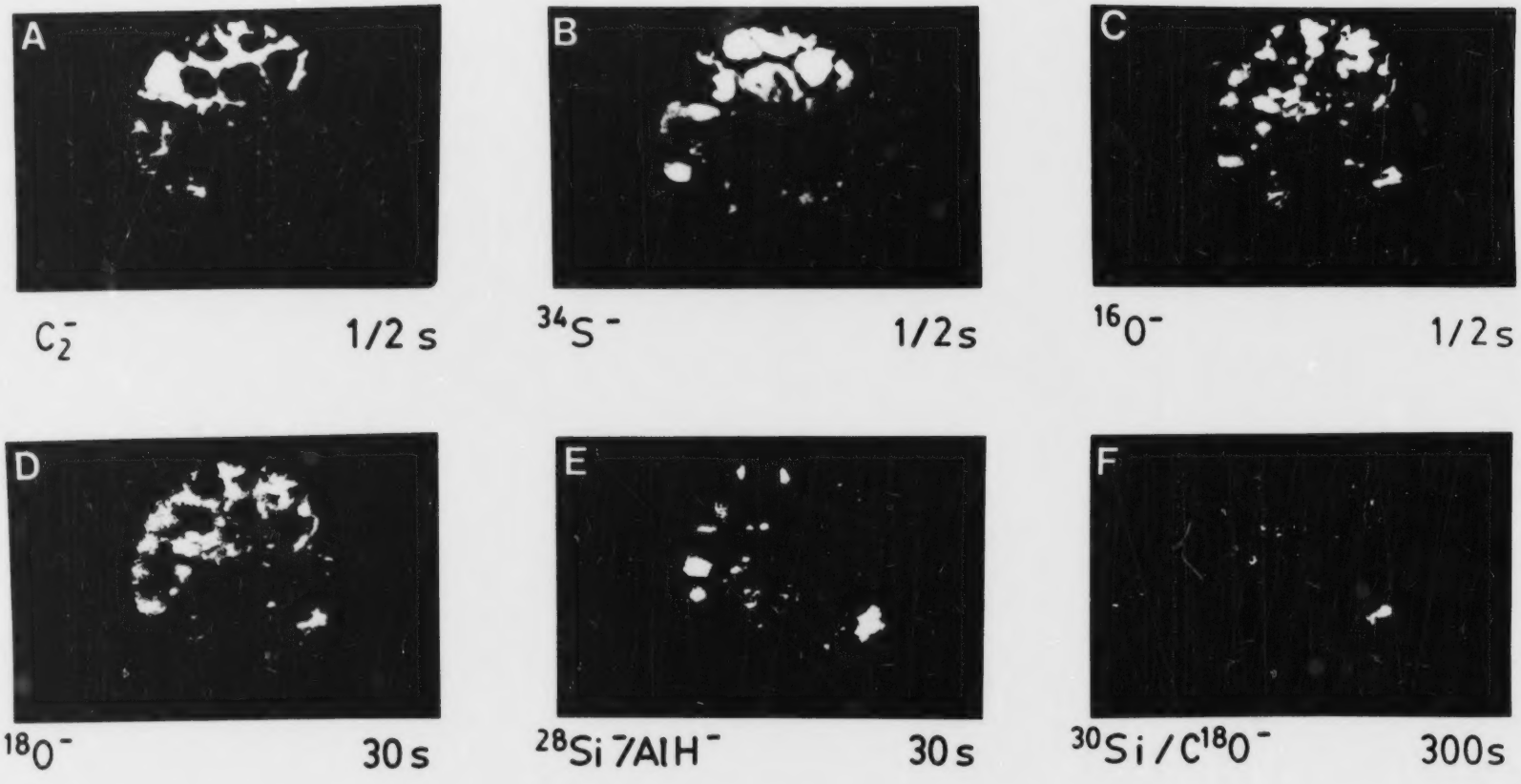
A
B
C
C_2^- 1/2 s
$^{34}S^-$ 1/2s
$^{16}O^-$ 1/2 s
D
E
F
$^{18}O^-$ 30 s
$^{28}Si^-/AlH^-$ 30 s
$^{30}Si/C^{18}O^-$ 300s

Fig. 4

C_2^- 1/2 sec

C_4^- 1 sec

CO^- 120 sec

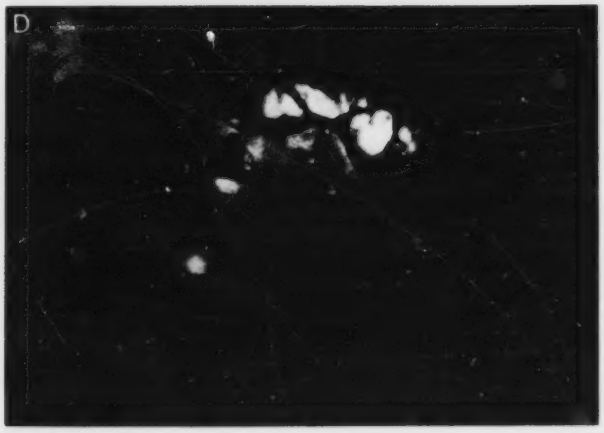

S^- 1/2 sec

CS^- 30 sec

Fig. 5

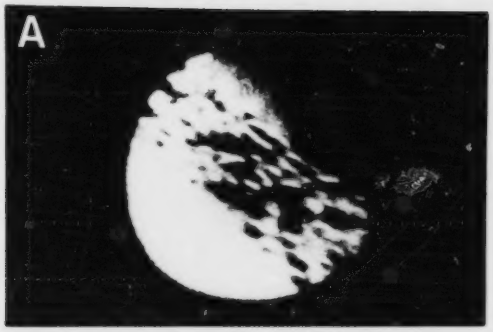

C_2^- 1/15 s

Al^+ 2 s

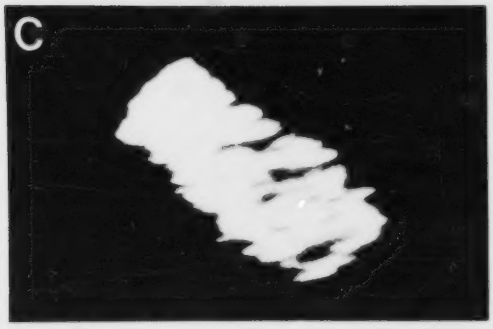

Si^+ 16 s

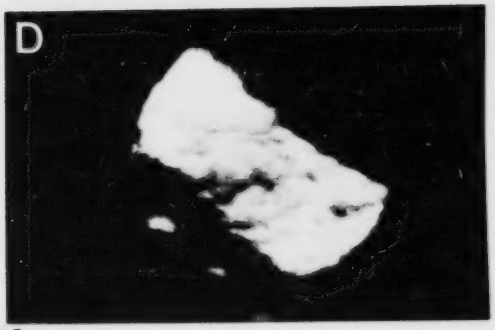

$^{16}O^-$ 1/4 s

$^{18}O^-$ 32 s

Fig. 6

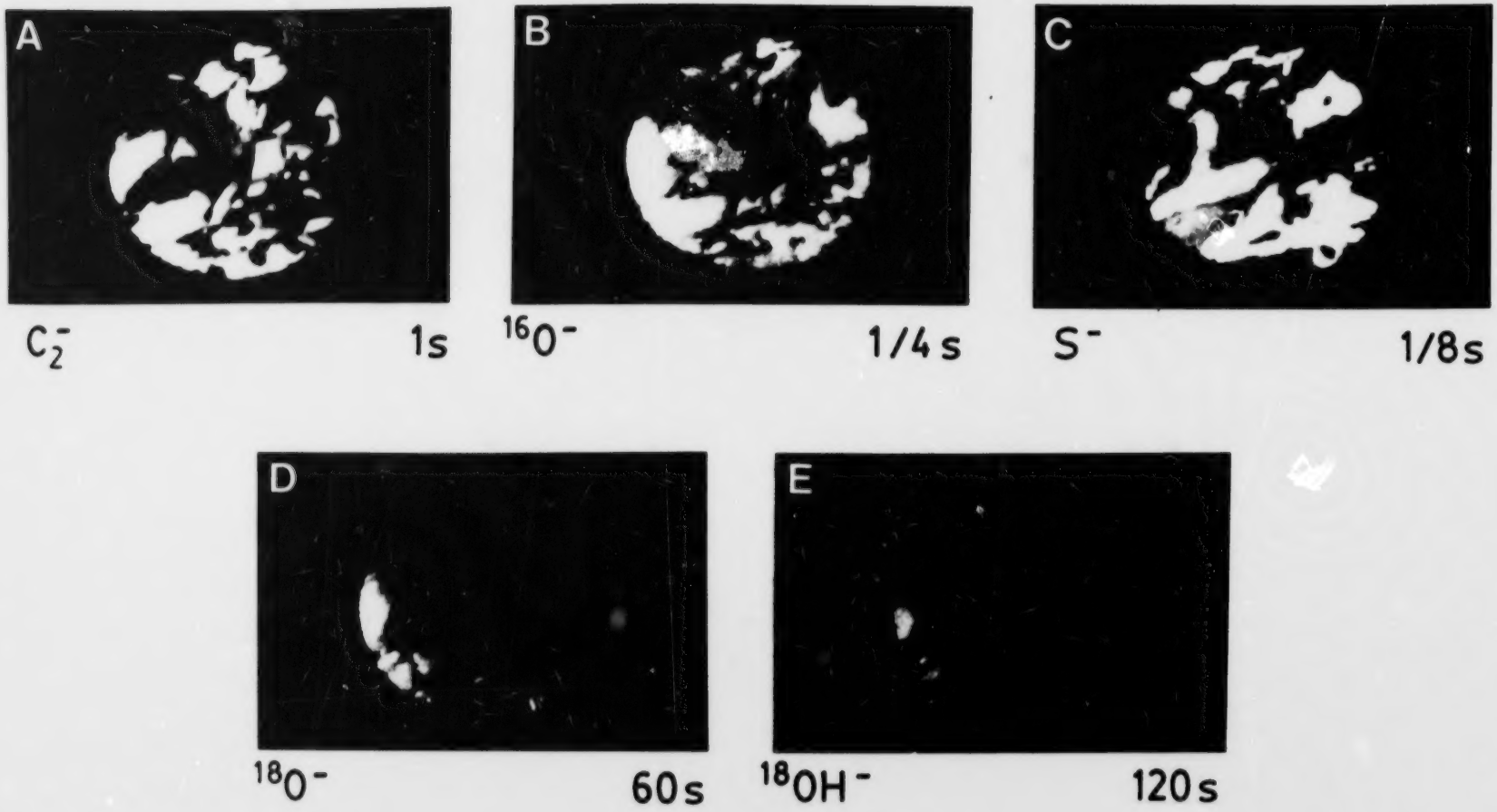

Fig. 7

Part A

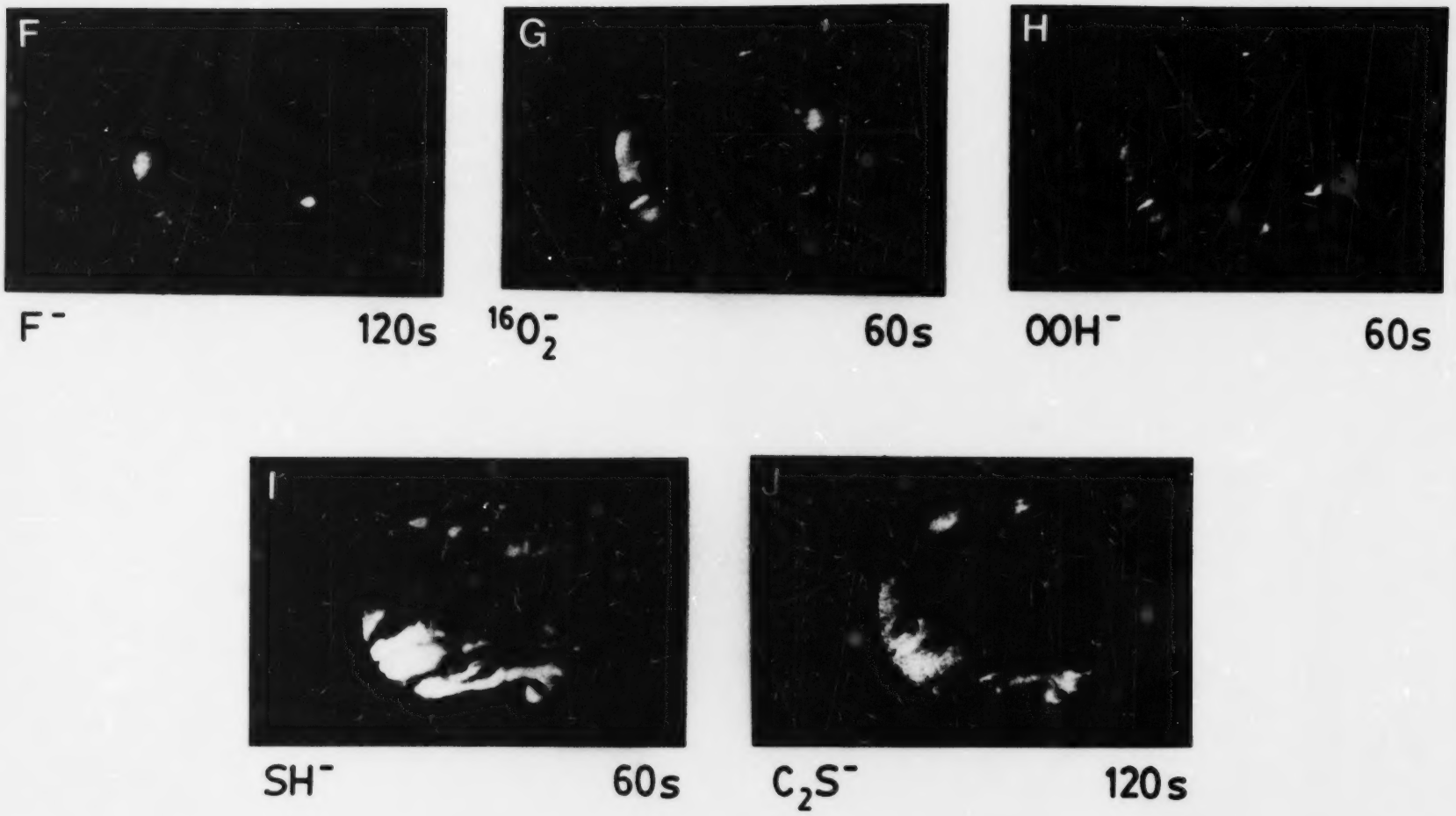

Fig. 7
Part B

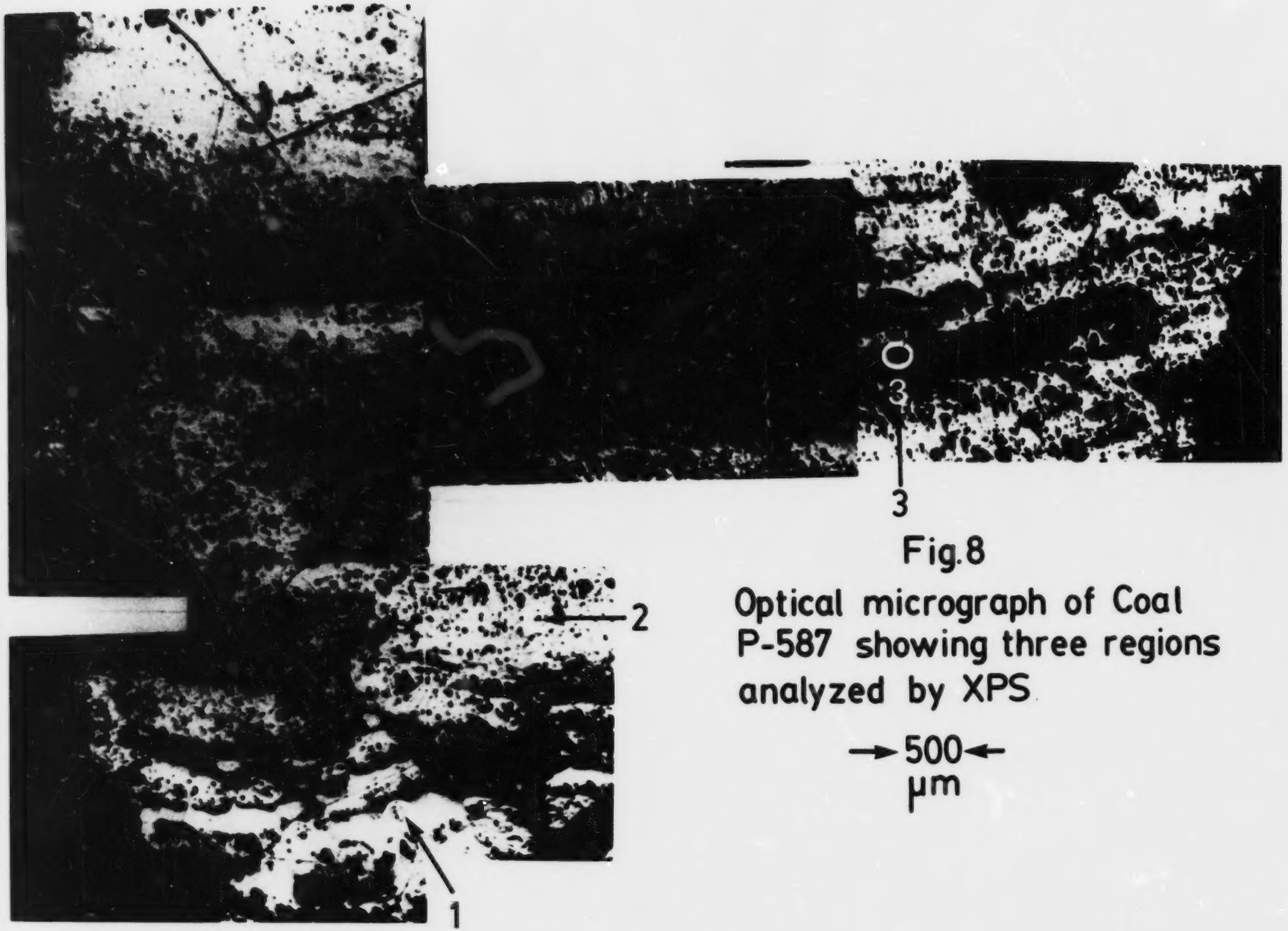

Fig.8

Optical micrograph of Coal P-587 showing three regions analyzed by XPS

→500←
μm

File: RRM3_003A	**Date:** 4/26/1986	**Spot Size:** 300 u	**Flood Gun:** 1.0 eV
Region 1	**Disc:** RRM02	**# of Scans:** 7	**Resolution:** 4
Description: P 587 REGION 1 (NO FEATURES)			**Operator:** NSM

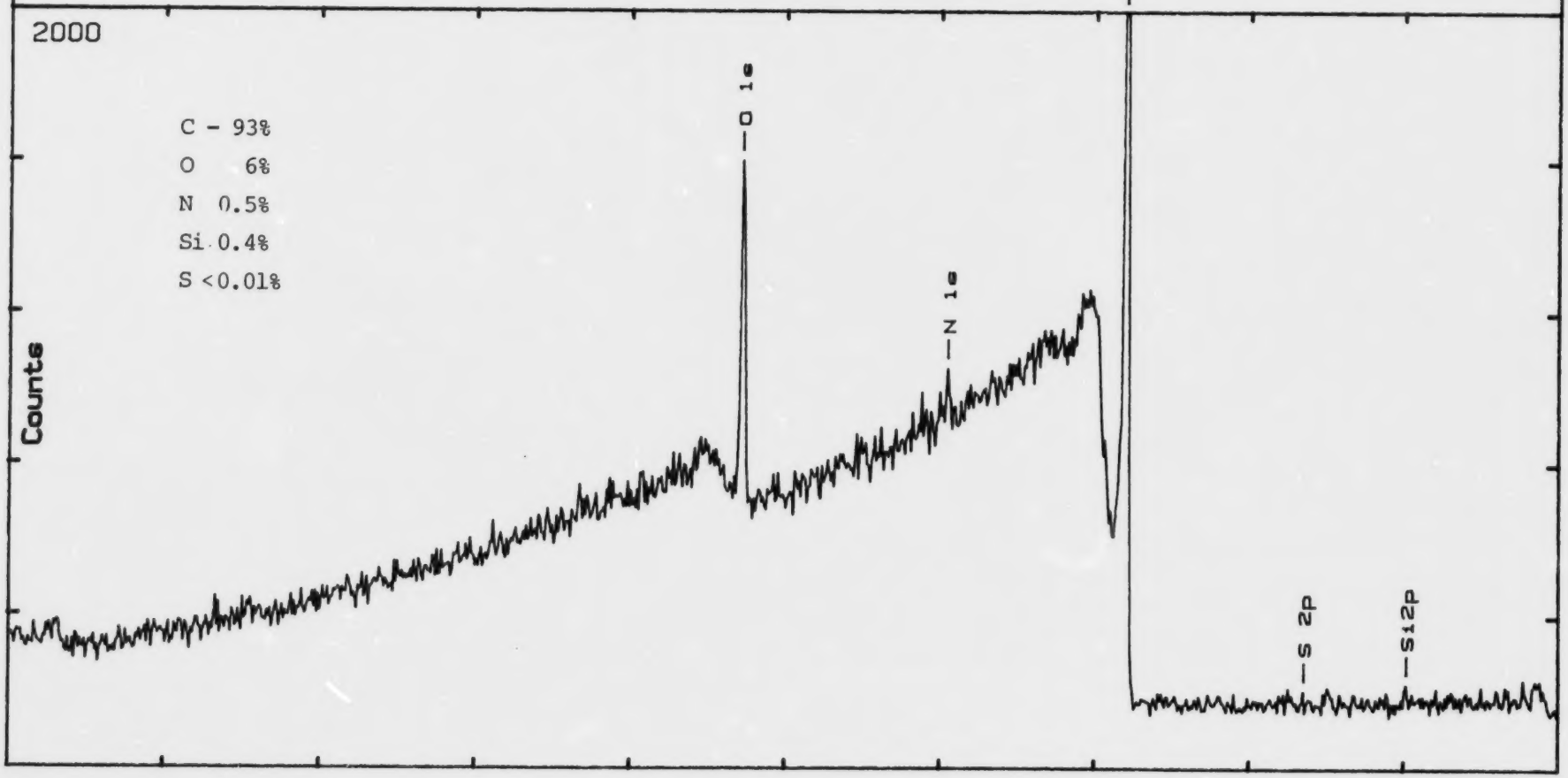

1000.0 **Binding Energy (eV)** 0.0

SURFACE SCIENCE WESTERN University of Western Ontario **Report #:** CANMET

File: RRM3_003B	Date: 4/26/1986	Spot Size: 300 u	Flood Gun: 1.0 eV
	Disc: RRM02	# of Scans: 30	Resolution: 4
Description: P 587 REGION 2			Operator: NSM

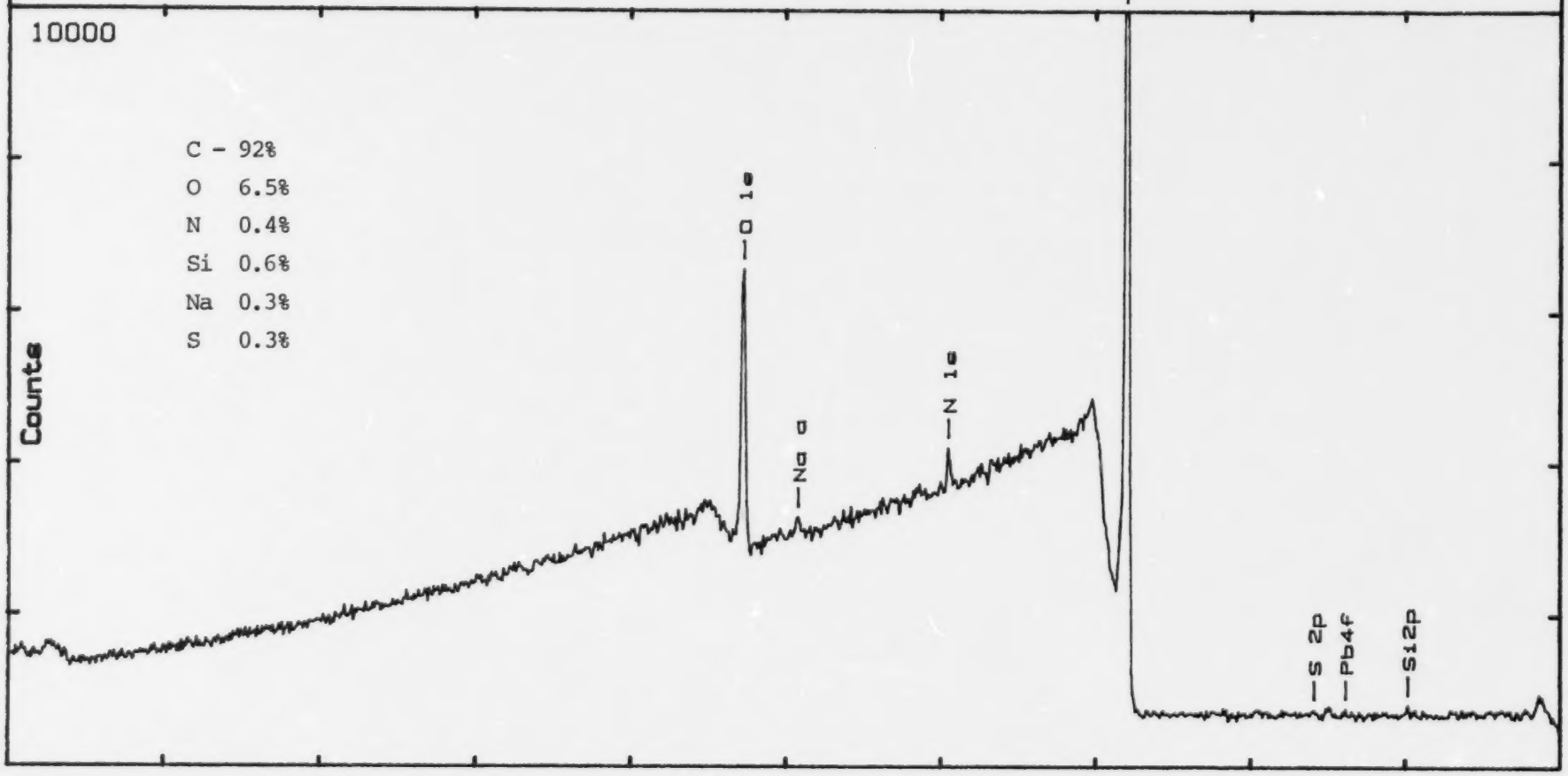

SURFACE SCIENCE WESTERN University of Western Ontario

Report #: CANMET

File: RRM3_004	Date: 4/26/1986	Spot Size: 300 u	Flood Gun: 1.0 eV
Region 1	Disc: RRM02	# of Scans: 25	Resolution: 4
Description: P 587 REGION 3(FUSINITE)			Operator: NSM

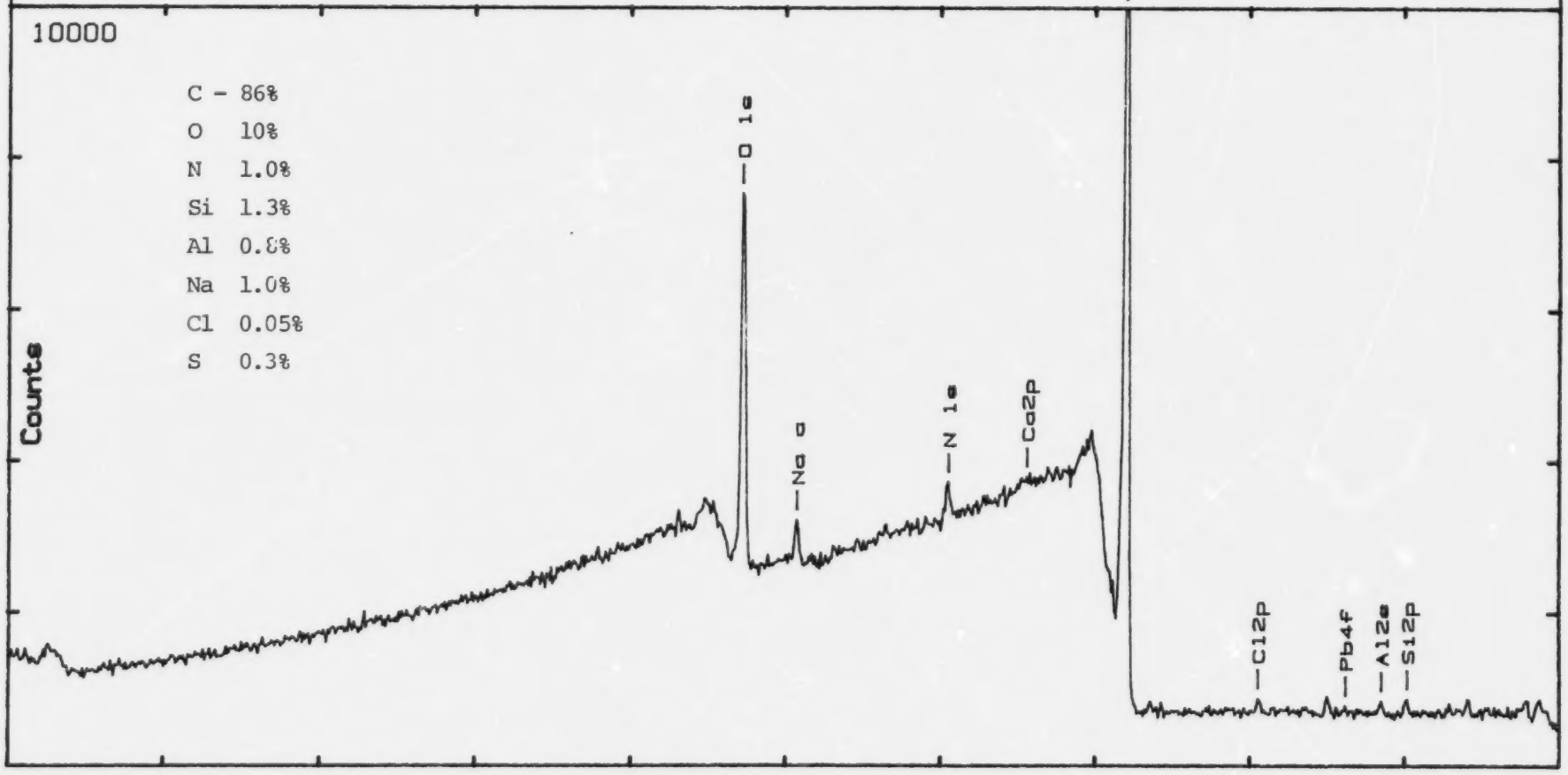

SURFACE SCIENCE WESTERN University of Western Ontario

Report #: CANMET

File: RRM3_003A	Date: 4/26/1986	Spot Size: 300 u	Flood Gun: 1.0 eV
Region 2	Disc: RRM02	# of Scans: 4	Resolution: 2
Description: P 587 REGION 1 (NO FEATURES)			Operator: NSM

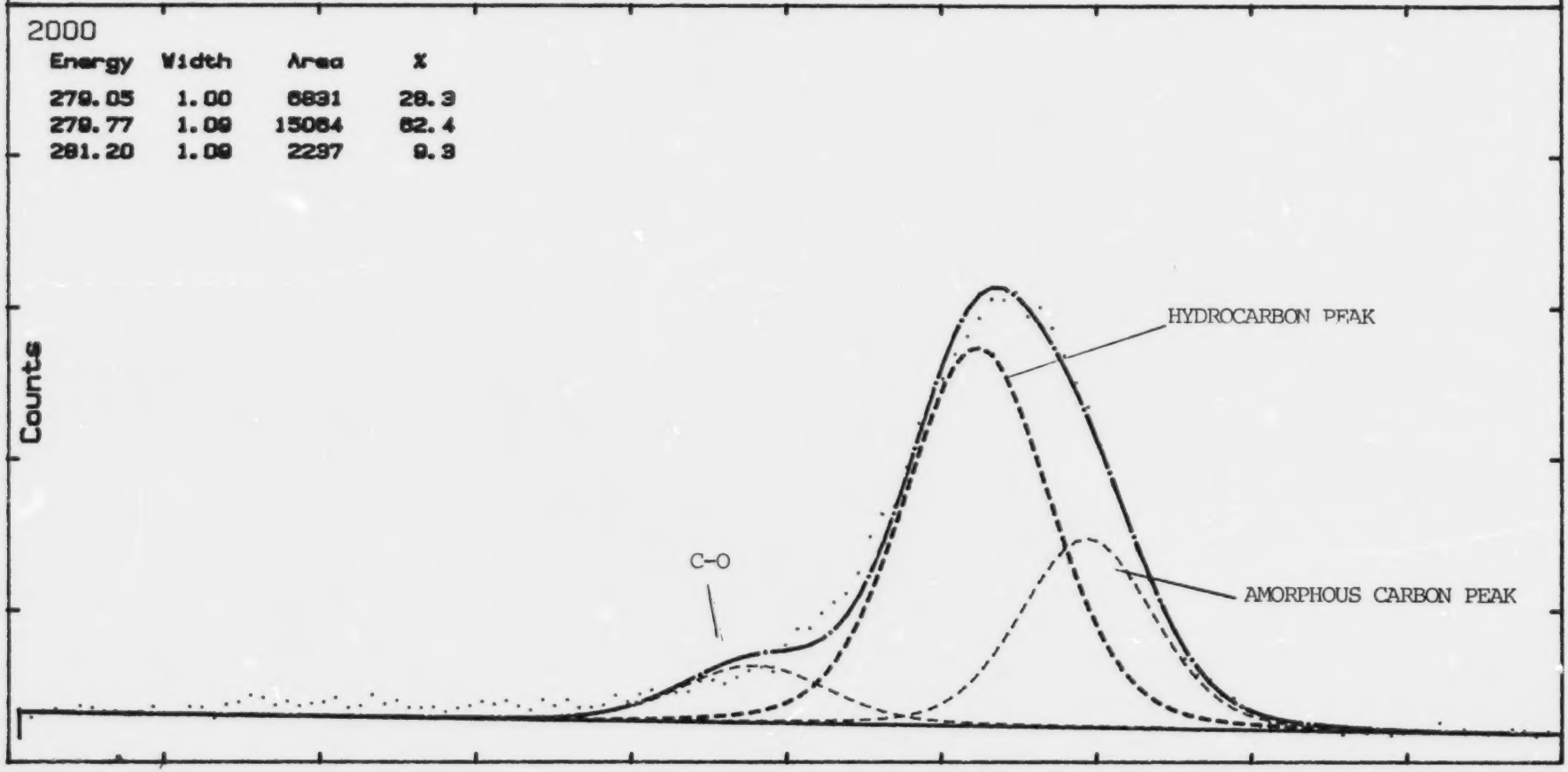

SURFACE SCIENCE WESTERN University of Western Ontario

Report #: CANMET

File: RRM3_004	Date: 4/26/1986	Spot Size: 300 u	Flood Gun: 1.0 eV
Region 2	Disc: RRM02	# of Scans: 20	Resolution: 2
Description: P 587 REGION 3(FUSINITE)			Operator: NSM

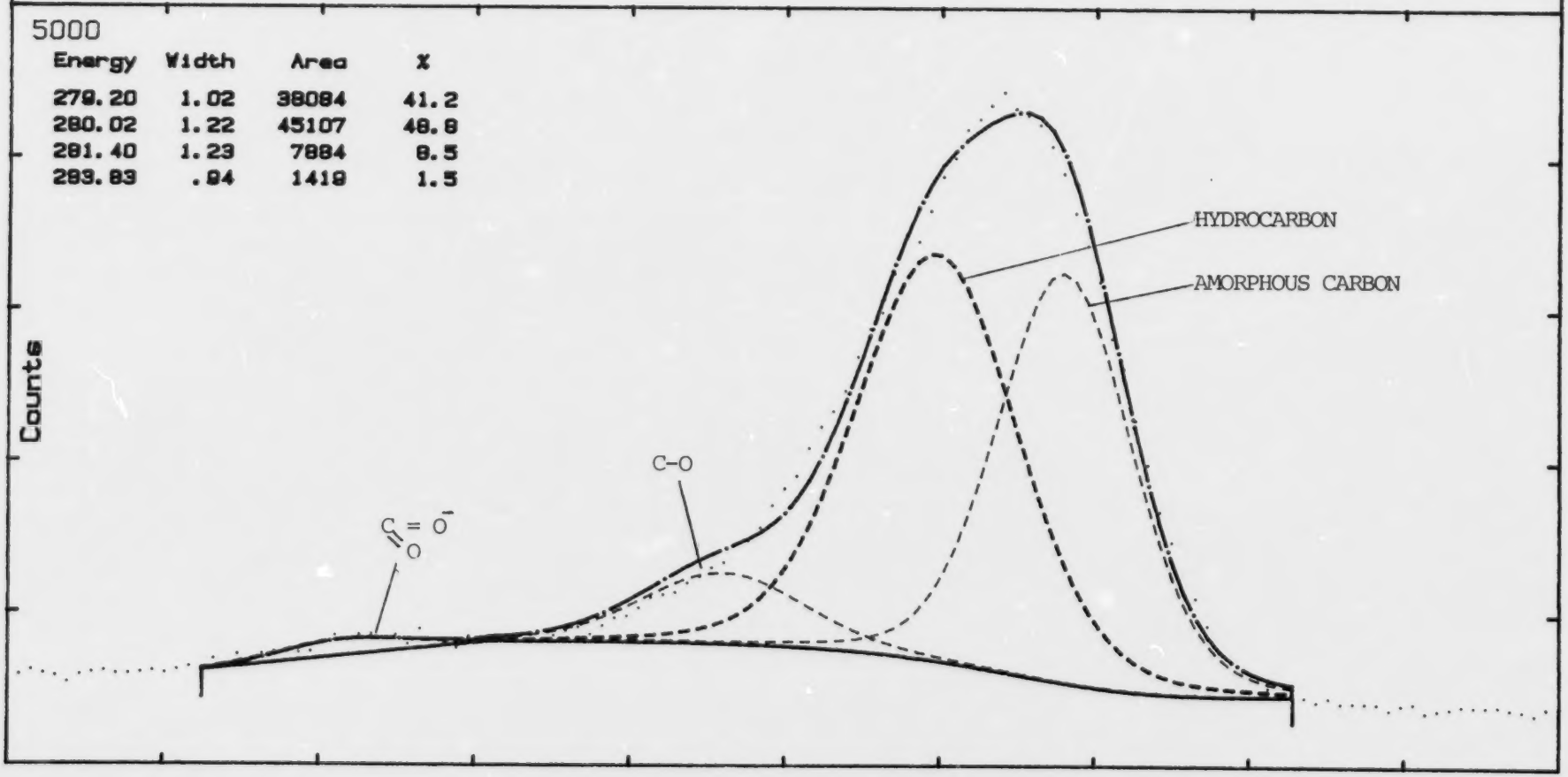

SURFACE SCIENCE WESTERN University of Western Ontario

Report #: CANMET

File: RRM3_11	Date: 5/3/1986	Spot Size: 300 u	Flood Gun: 1.0 eV
Region 1	Disc: RRM02	# of Scans: 20	Resolution: 4
Description: P 587 OXIDIZED FUSINITE			Operator: NSM

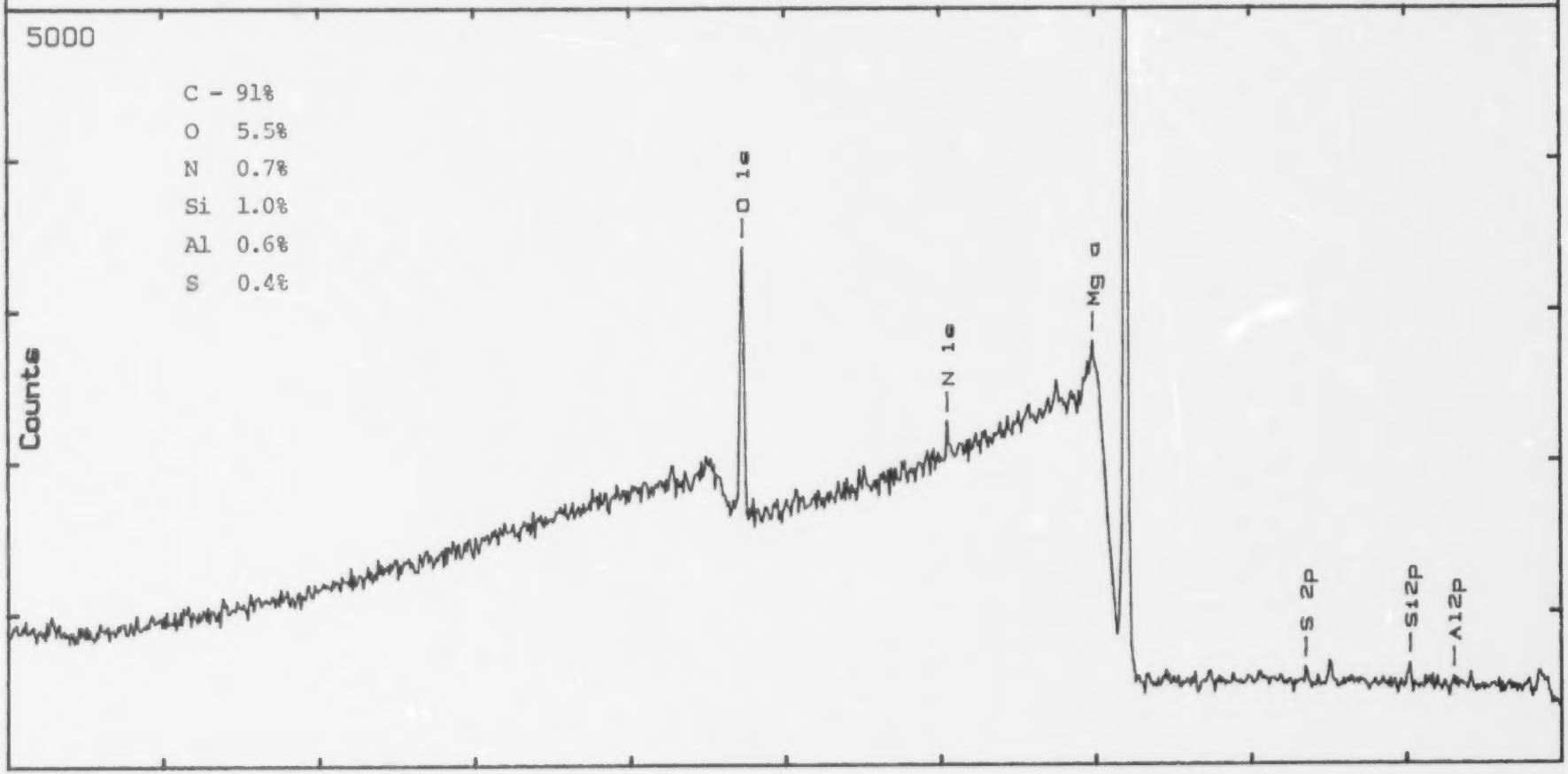

SURFACE SCIENCE WESTERN University of Western Ontario

Report #: CANMET

File: RRM3_11	Date: 5/3/1986	Spot Size: 300 u	Flood Gun: 1.0 eV
Region 2	Disc: RRM02	# of Scans: 20	Resolution: 2

Description: P 587 OXIDIZED FUSINITE **Operator:** NSM

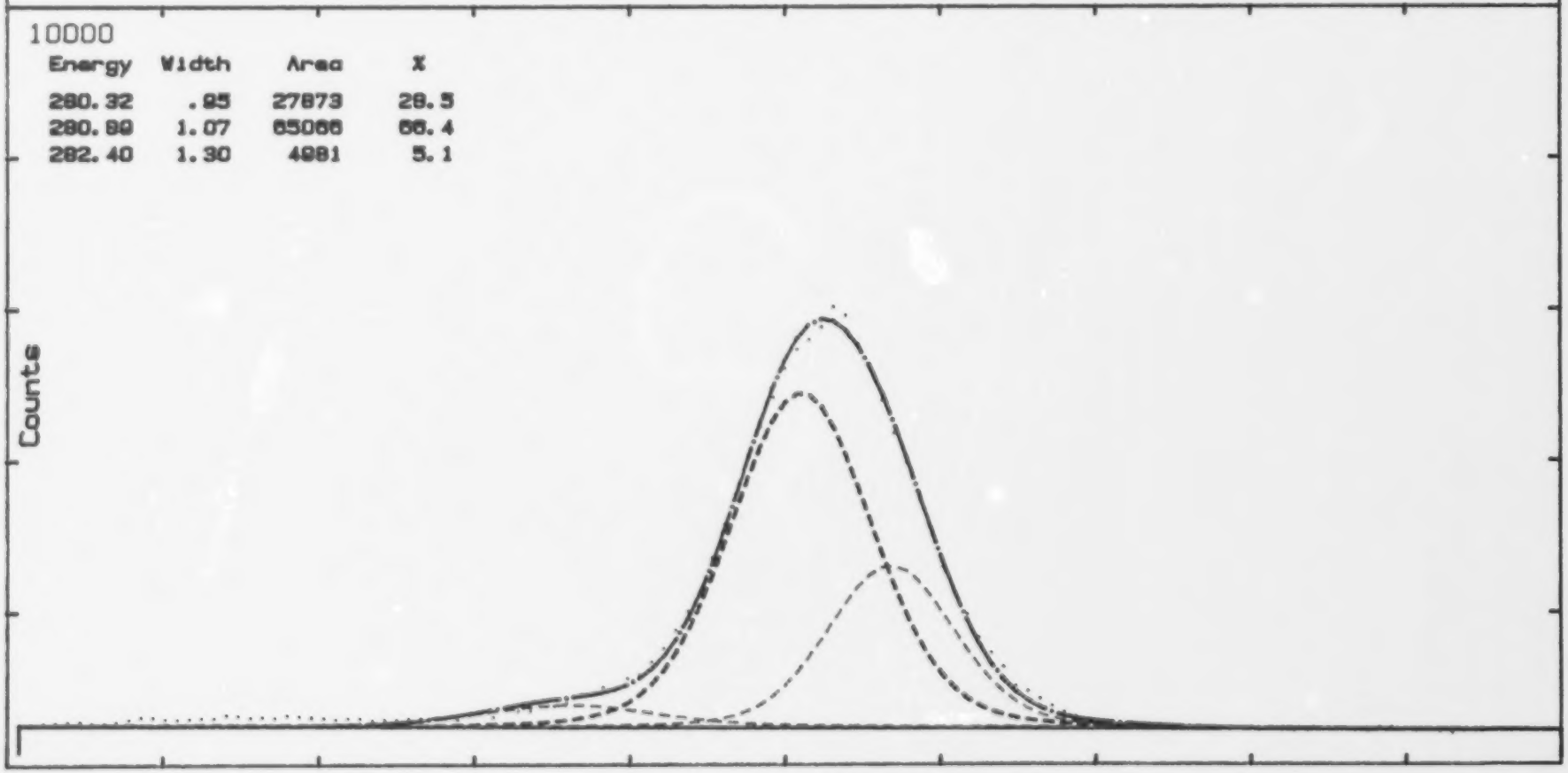

SURFACE SCIENCE WESTERN University of Western Ontario **Report #:** CANMET

File: RRM2_10	Date: 4/17/1986	Spot Size: 600 u	Flood Gun: 3.0 eV
Region 1	Disc: RRM01	# of Scans: 30	Resolution: 4
Description: P-250			Operator: NSM

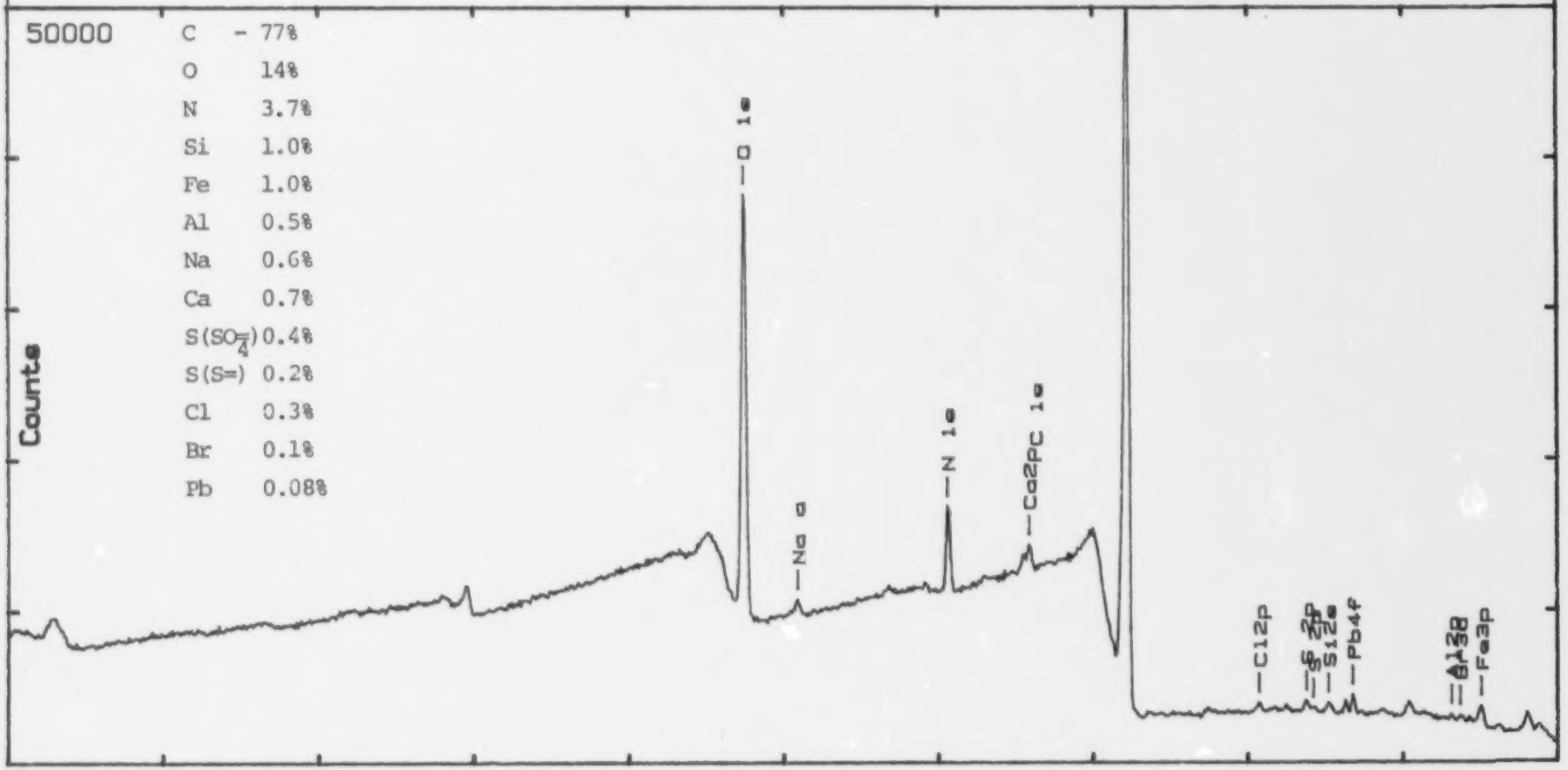

1000.0 **Binding Energy (eV)** 0.0

SURFACE SCIENCE WESTERN University of Western Ontario **Report #:** CANMET

File: RRM2_10	Date: 4/17/1986	Spot Size: 600 u	Flood Gun: 3.0 eV
Region 2	Disc: RRM01	# of Scans: 30	Resolution: 2
Description: P-250			Operator: NSM

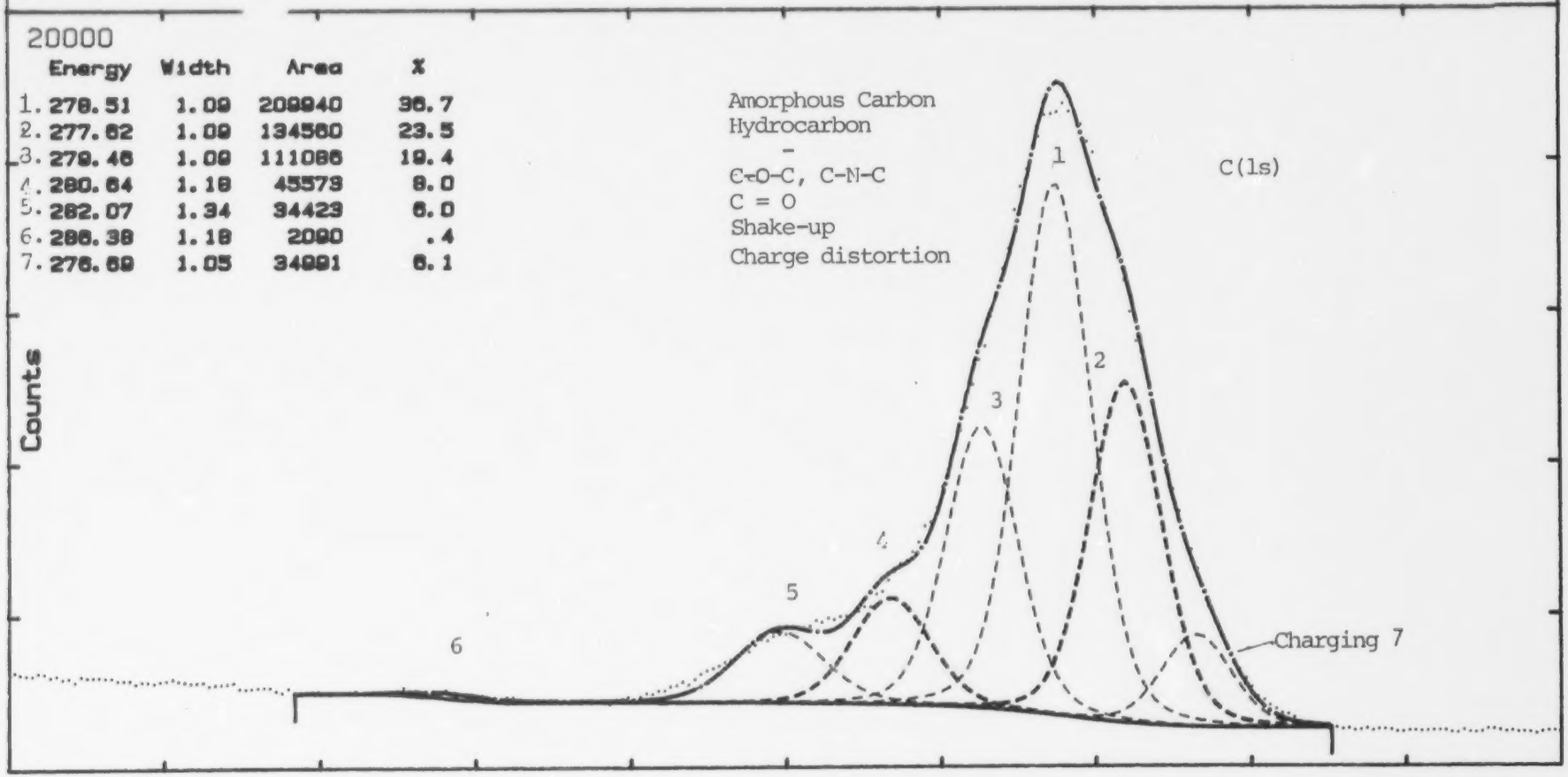

SURFACE SCIENCE WESTERN University of Western Ontario

Report #: CANMET

File: RRM3_12	**Date:** 5/3/1986	**Spot Size:** 300 u	**Flood Gun:** 1.0 eV
Region 1	**Disc:** RRM02	**# of Scans:** 20	**Resolution:** 4
Description: P-250 (Oxidized)			**Operator:** NSM

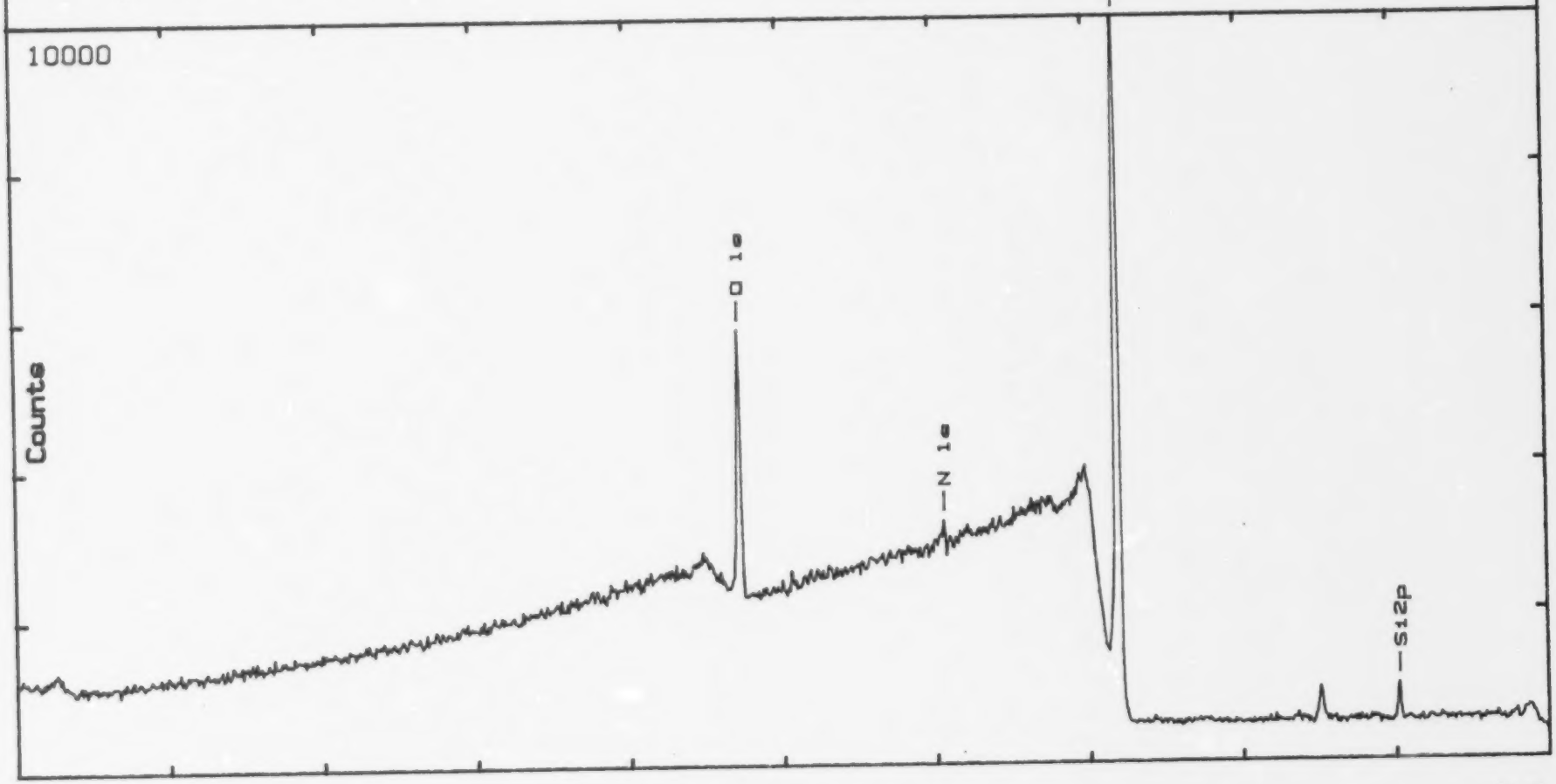

SURFACE SCIENCE WESTERN University of Western Ontario

Report #: CANMET

(a)

File: RRM3_12	Date: 5/3/1986	Spot Size: 300 u	Flood Gun: 1.0 eV
Region 2	Disc: RRM02	# of Scans: 20	Resolution: 2
Description: P-250 (Oxidized)			Operator: NSM

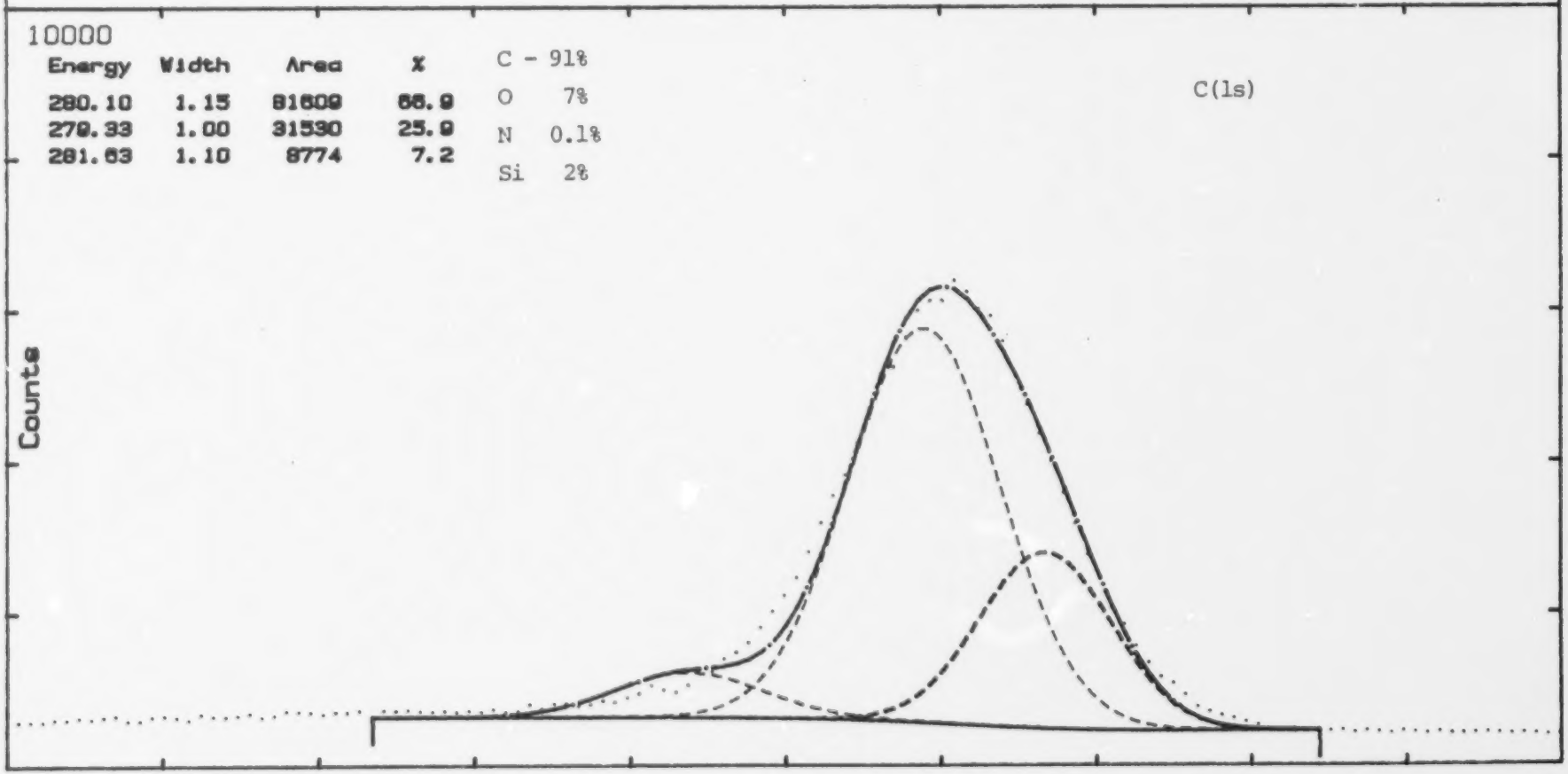

SURFACE SCIENCE WESTERN University of Western Ontario

Report #: CANMET

File: RRM3_002	Date: 4/25/1986	Spot Size: 1000 u	Flood Gun: 1.0 eV
Region 1	Disc: RRM02	# of Scans: 20	Resolution: 4

Description:

Operator: NSM

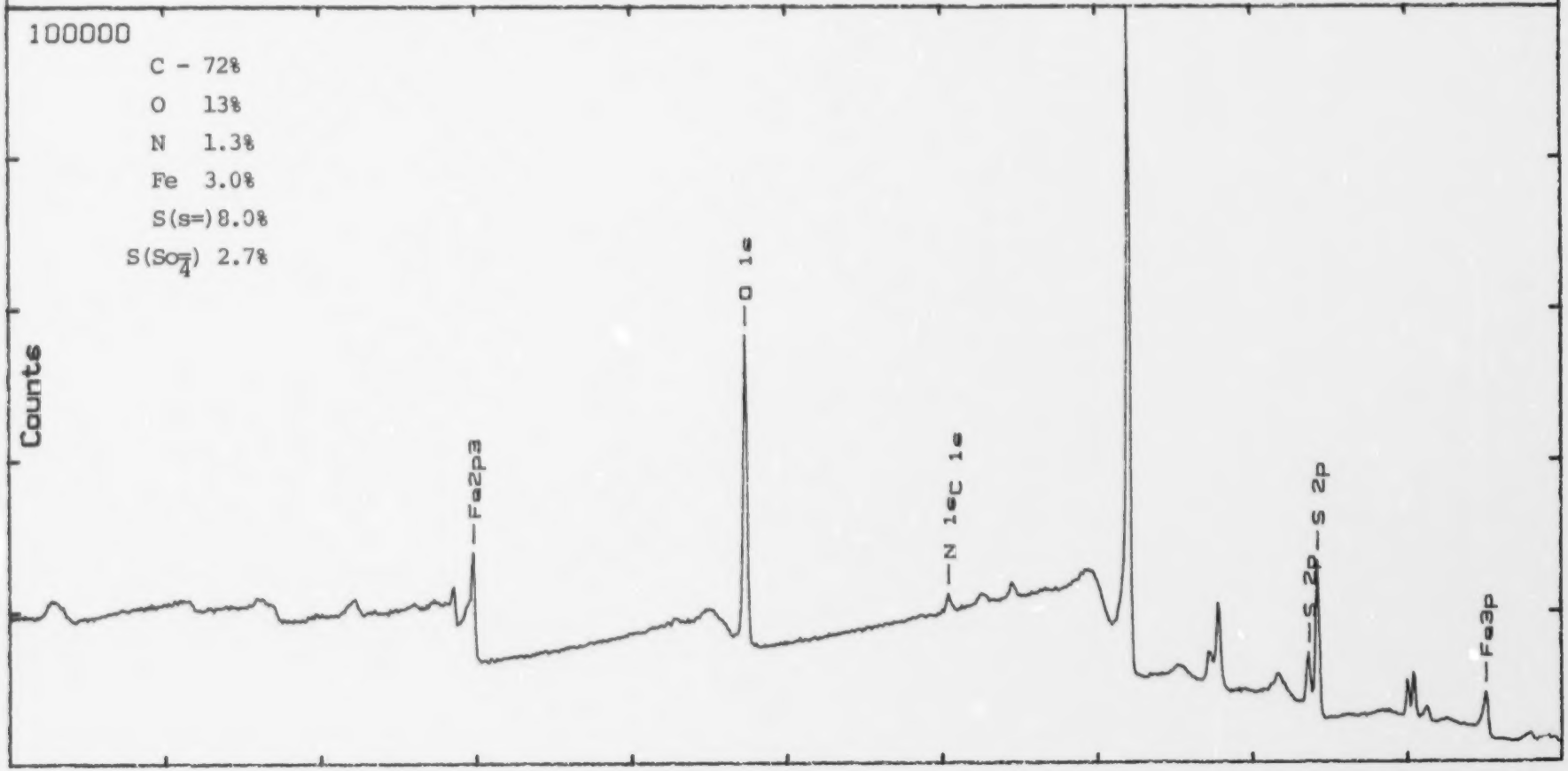

SURFACE SCIENCE WESTERN University of Western Ontario

Report #: CANMET

File: RRM3_002A	Date: 4/25/1986	Spot Size: 300 u	Flood Gun: 1.0 eV
Region 3	Disc: RRM02	# of Scans: 50	Resolution: 2
Description: PYRITE COAL CLEAVE			Operator: NSM

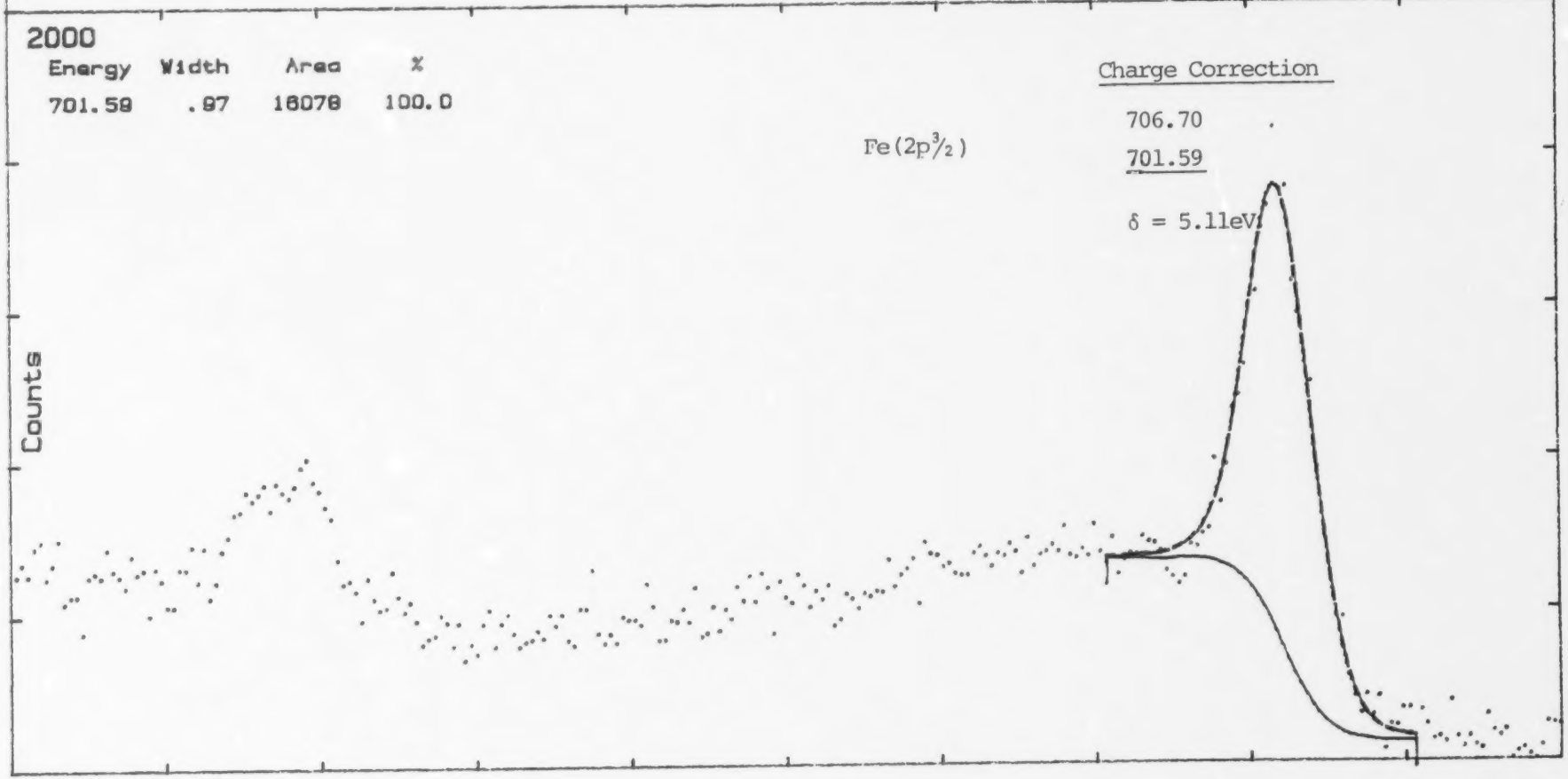

SURFACE SCIENCE WESTERN University of Western Ontario

File: RRM3_002A	Date: 4/25/1986	Spot Size: 300 u	Flood Gun: 1.0 eV
Region 1	Disc: RRM02	# of Scans: 50	Resolution: 2
Description: PYRITE COAL CLEAVE			Operator: NSM

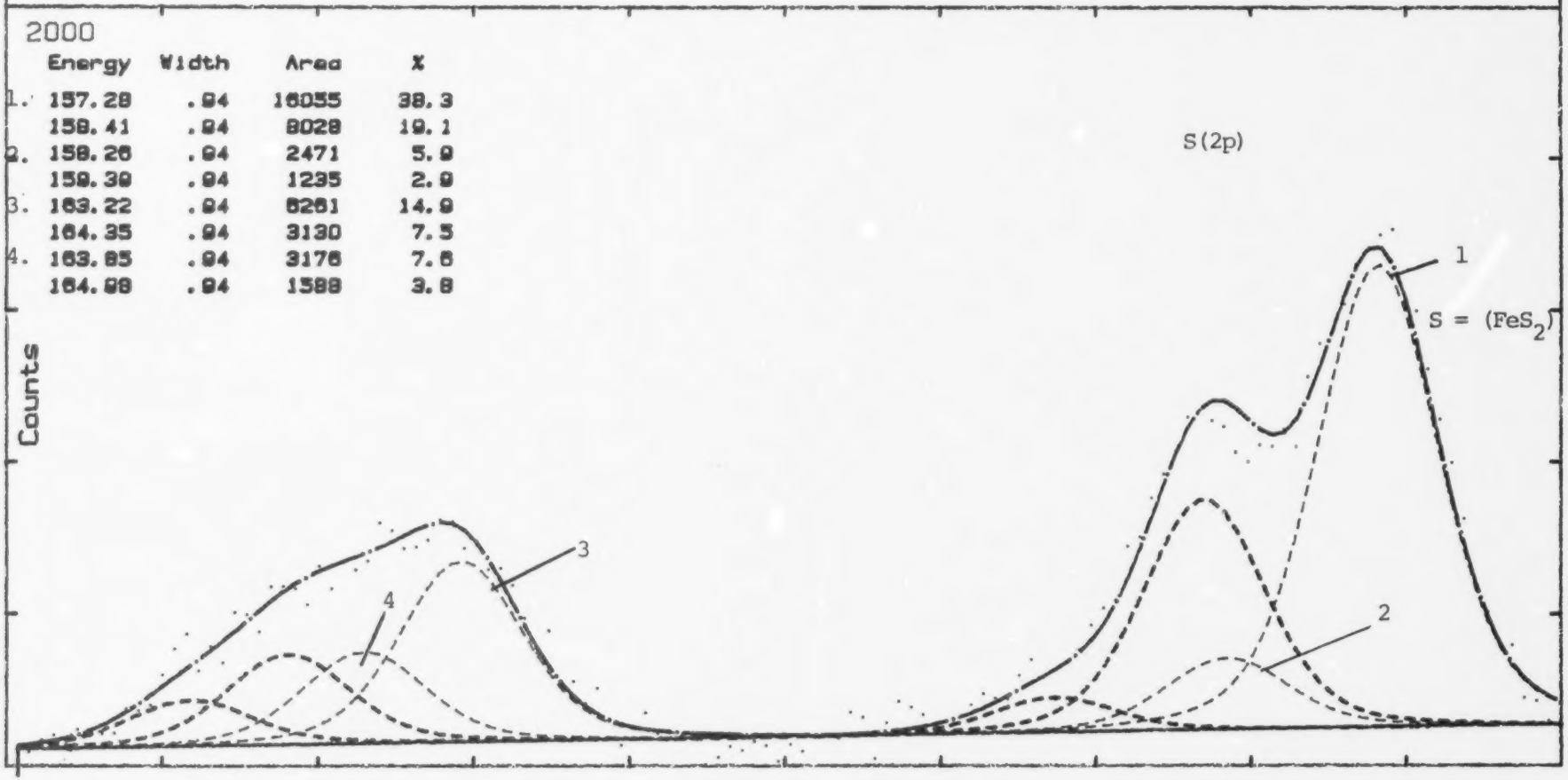

SURFACE SCIENCE WESTERN University of Western Ontario

Report #: CANMET

File: RRM3_002	Date: 4/25/1986	Spot Size: 300 u	Flood Gun: 1.0 eV
Region 2	Disc: RRM02	# of Scans: 20	Resolution: 2
Description:			Operator: NSM

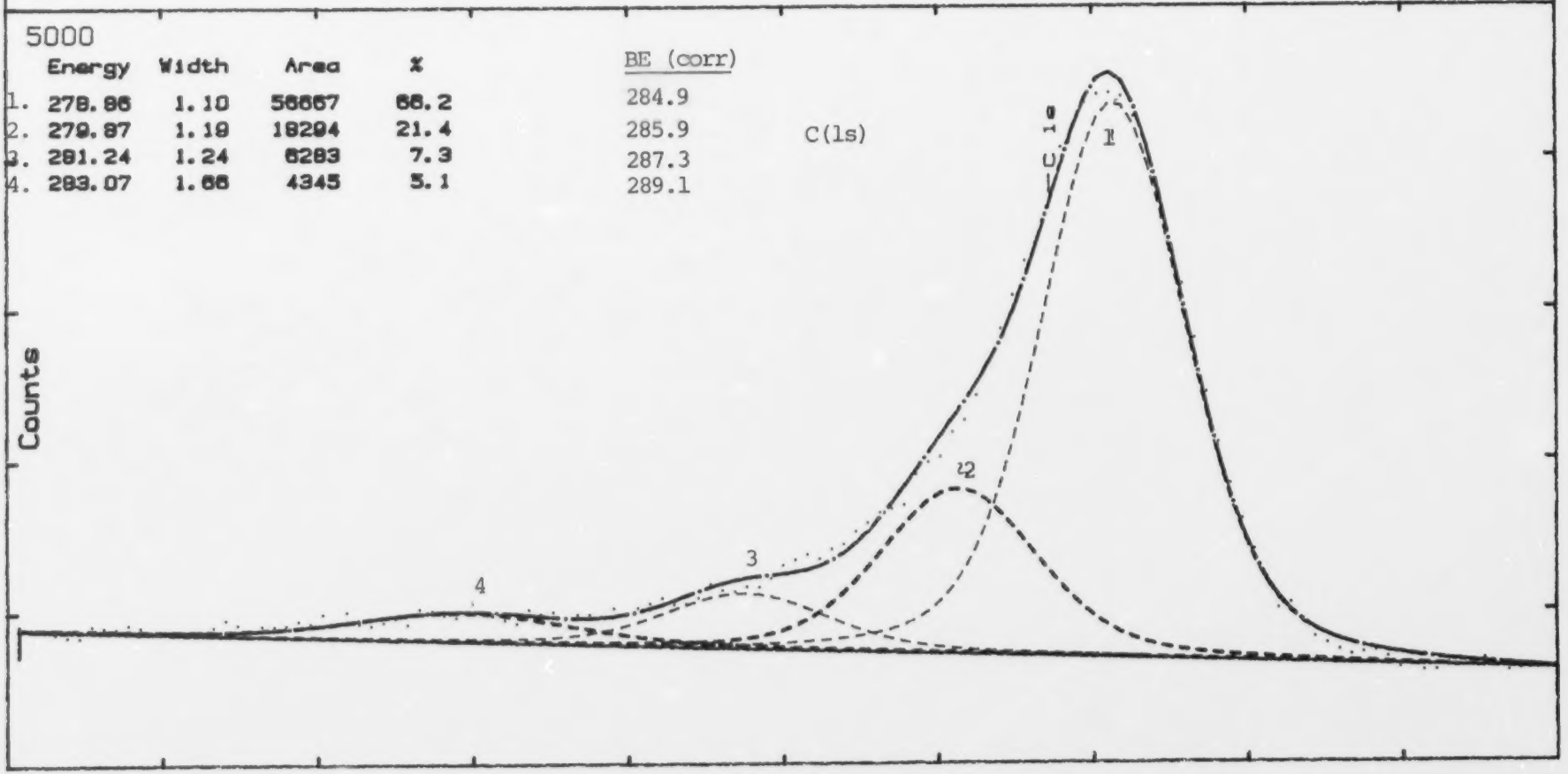

286.0 **Binding Energy (eV)** 276.0

SURFACE SCIENCE WESTERN University of Western Ontario **Report #:** CANMET

File: RRM2_06	Data: 4/16/1986	Spot Size: 600 u	Flood Gun: 1.0 eV
Region 2	Disc: RRM01	# of Scans: 30	Resolution: 4
Description: PYRITE COAL 2 FRACTURED SIDE			Operator: NSM

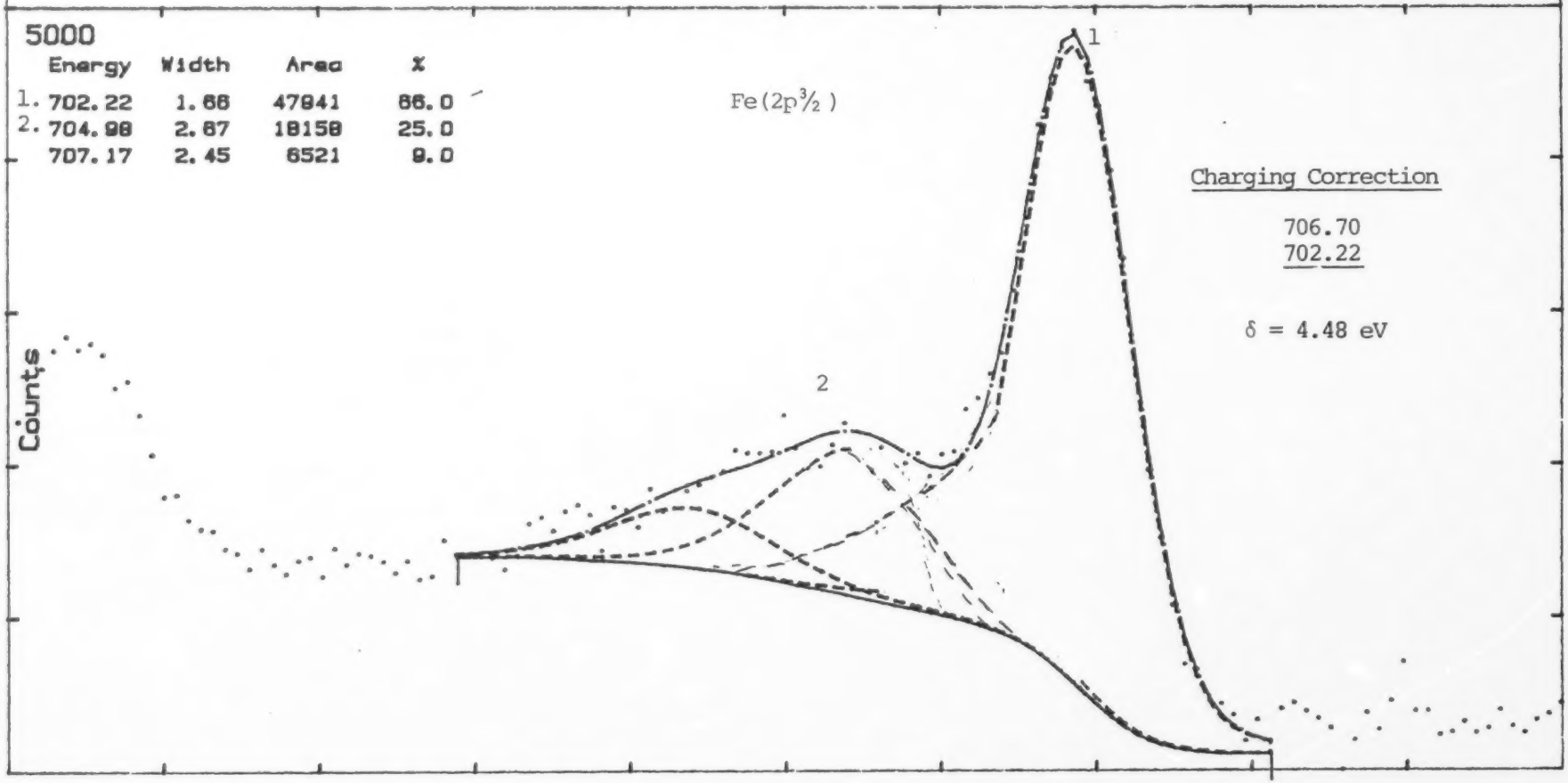

SURFACE SCIENCE WESTERN University of Western Ontario

File: RRM2_06	Date: 4/16/1986	Spot Size: 600 u	Flood Gun: 1.0 eV
Region 4	Disc: RRM01	# of Scans: 100	Resolution: 2
Description: PYRITE COAL 2 FRACTURED SIDE			Operator: NSM

20000

	Energy	Width	Area	%
1.	157.08	.96	40619	15.6
	158.21	.94	20309	7.8
2,	157.83	.97	115869	44.4
	158.96	.96	57935	22.2
3,	159.48	.96	17434	6.7
	160.61	.96	8717	3.3

S(2p) δ = 4.48 eV

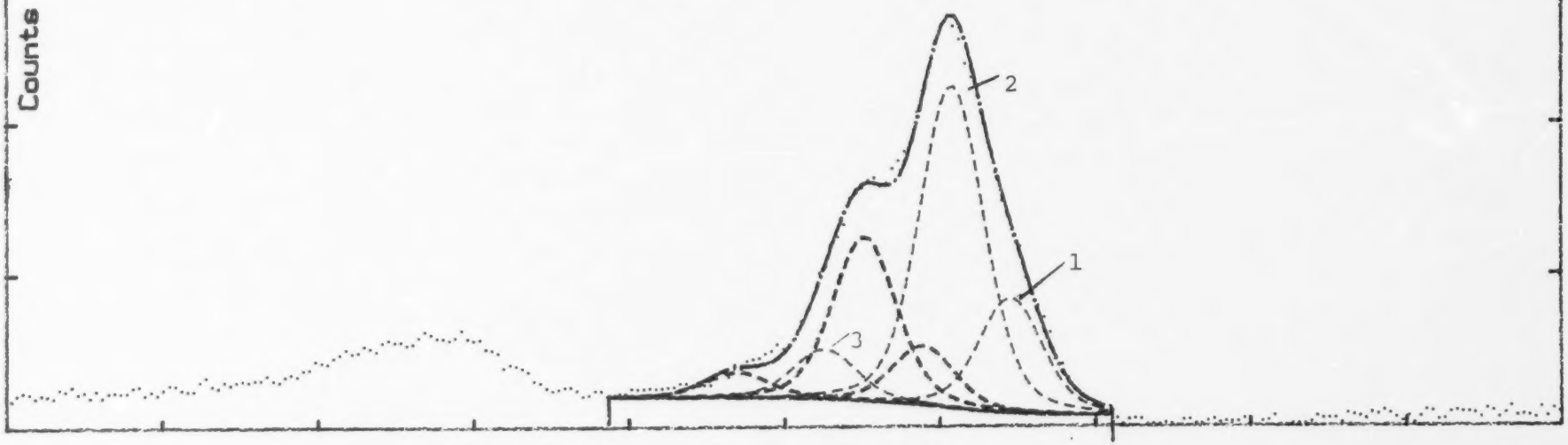

170.0 **Binding Energy (eV)** 150.0

SURFACE SCIENCE WESTERN University of Western Ontario **Report #:** CANMET

File: RRM2_06	Date: 4/16/1986	Spot Size: 600 u	Flood Gun: 1.0 eV
Region 4	Disc: RRM01	# of Scans: 100	Resolution: 2

Description: PYRITE COAL 2 FRACTURED SIDE **Operator:** NSM

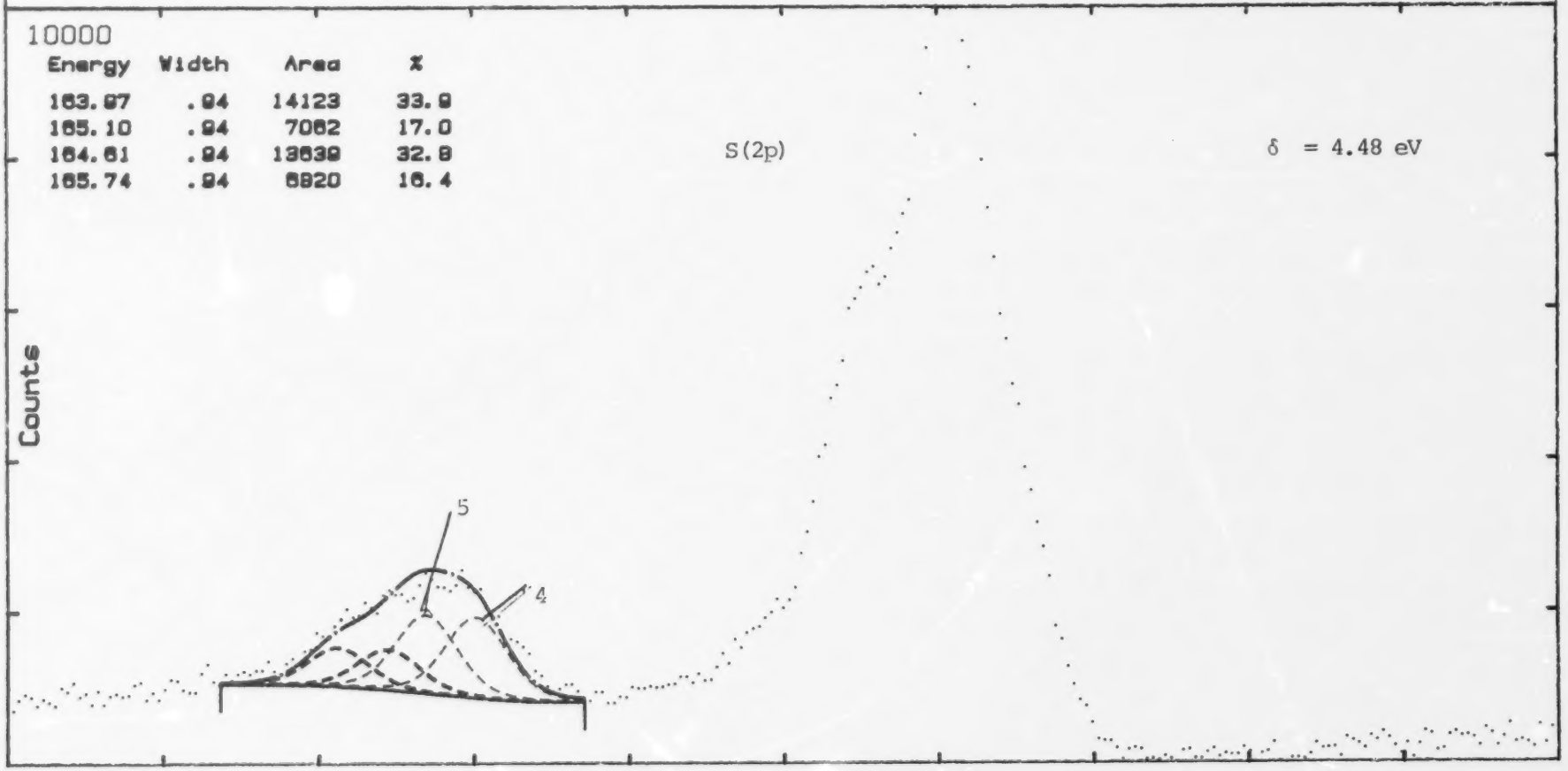

SURFACE SCIENCE WESTERN University of Western Ontario **Report #:** CANMET

File: RRM2_06	Date: 4/16/1986	Spot Size: 600 u	Flood Gun: 1.0 eV
Region 5	Disc: RRM01	# of Scans: 50	Resolution: 2

Description: PYRITE COAL 2 FRACTURED SIDE Operator: NSM

50000

	Energy	Width	Area	%	Assignment
1	279.82	1.09	238830	22.9	Camorph
2	280.27	1.09	261920	25.4	Hydrocarbon
3	281.10	1.09	210980	20.4	C - S
4	282.00	1.09	147126	14.3	C - O
5	282.89	1.09	97983	9.5	C = O
6	283.87	1.09	56544	5.5	C = O
7	284.84	1.09	20648	2.0	O

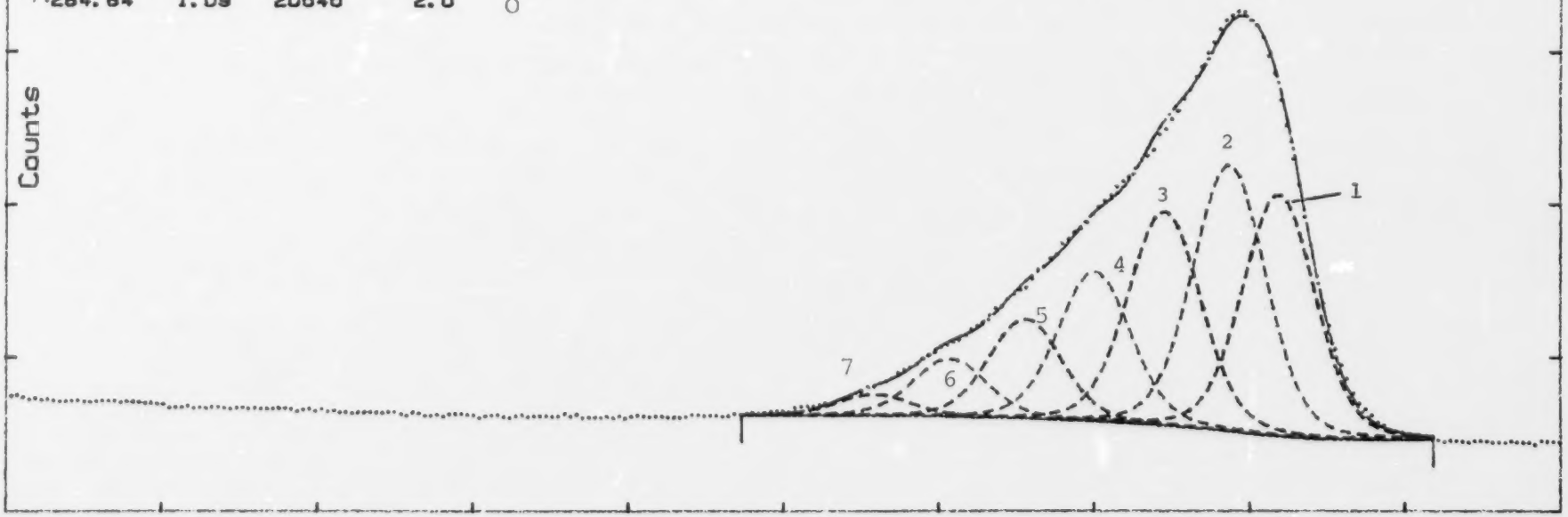

296.0 Binding Energy (eV) 276.0

SURFACE SCIENCE WESTERN University of Western Ontario

File: RRM3_16	Date: 6/23/1986	Spot Size: 1000 u	Flood Gun: 1.0 eV
Region 1	Disc: RRM02	# of Scans: 2	Resolution: 4

Description: FUSINITE LOOKING PERPENDICULAR TO CLEAVED SURFACE (ie. IN CROSS-SECTION) **Operator:** JRM

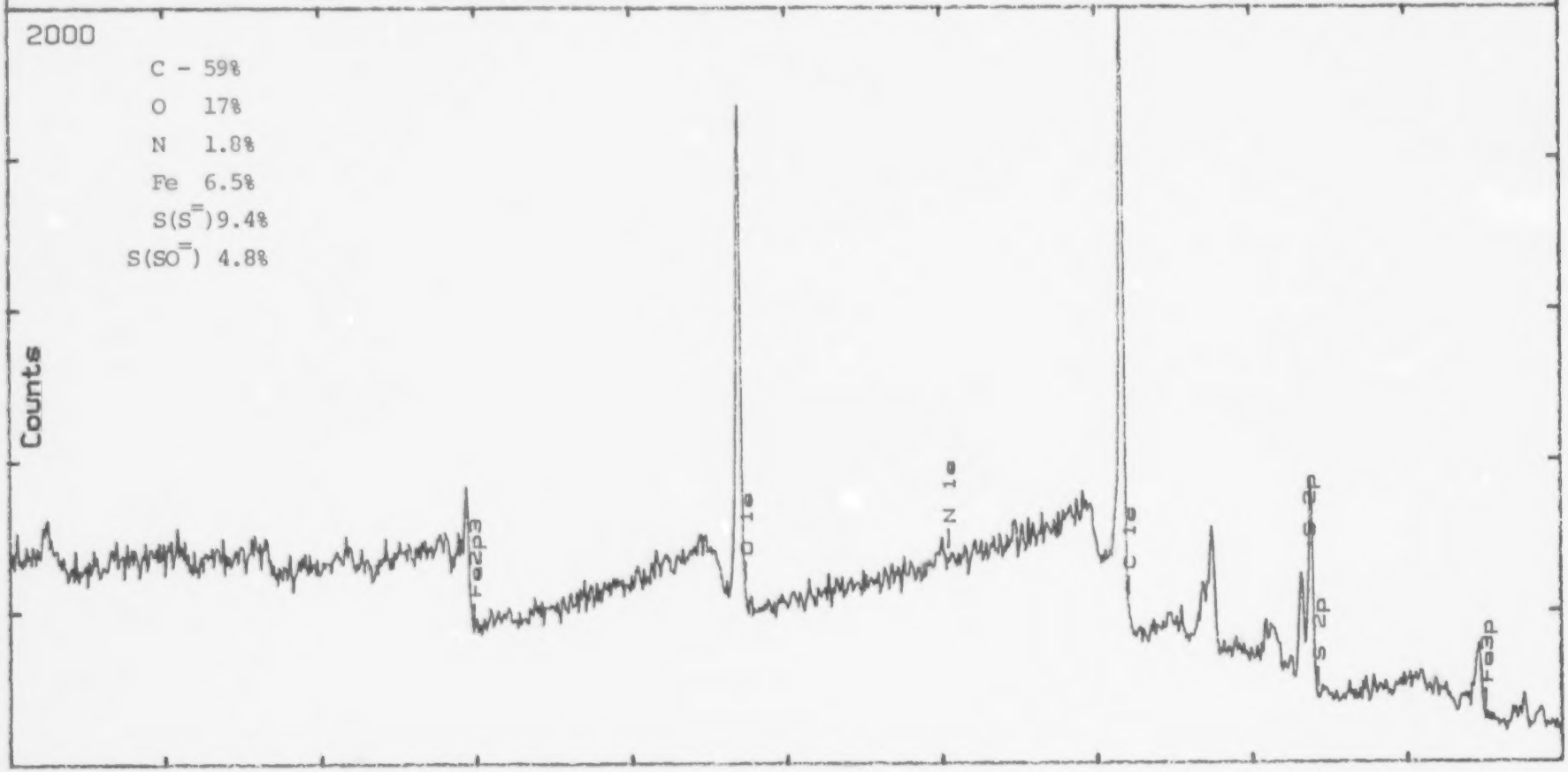

SURFACE SCIENCE WESTERN University of Western Ontario **Report #:** CANMET

File: RRM3_16A	**Date:** 6/24/1986	**Spot Size:** 1000 u	**Flood Gun:** 1.0 eV
Region 1	**Disc:** RRM02	**# of Scans:** 2	**Resolution:** 4
Description: FUSINITE RRM3_16 AFTER 15 HRS. EXPOSURE TO AIR AT 70 degrees C			**Operator:** JRM

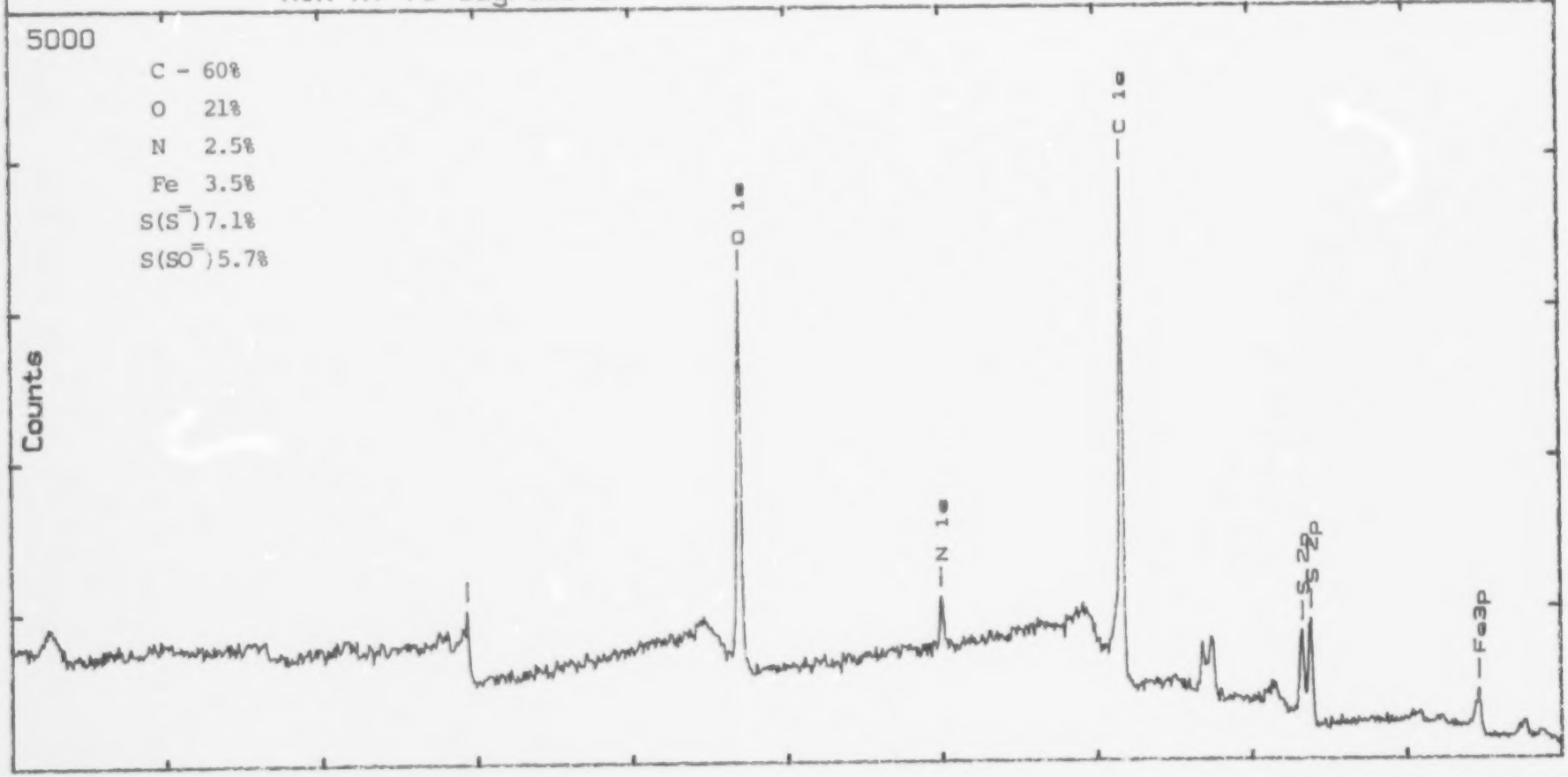

SURFACE SCIENCE WESTERN University of Western Ontario

Report #: CANMET

File: RRM3_16B	Date: 7/7/1986	Spot Size: 300 u	Flood Gun: 1.0 eV
Region 2	Disc: RRM02	# of Scans: 20	Resolution: 2

Description: FUSINITE RRM3_16(RRM3_16A) AFTER 309 HRS. OF ADDITIONAL EXPOSURE TO AIR AT 70 deg. C

Operator: JRM

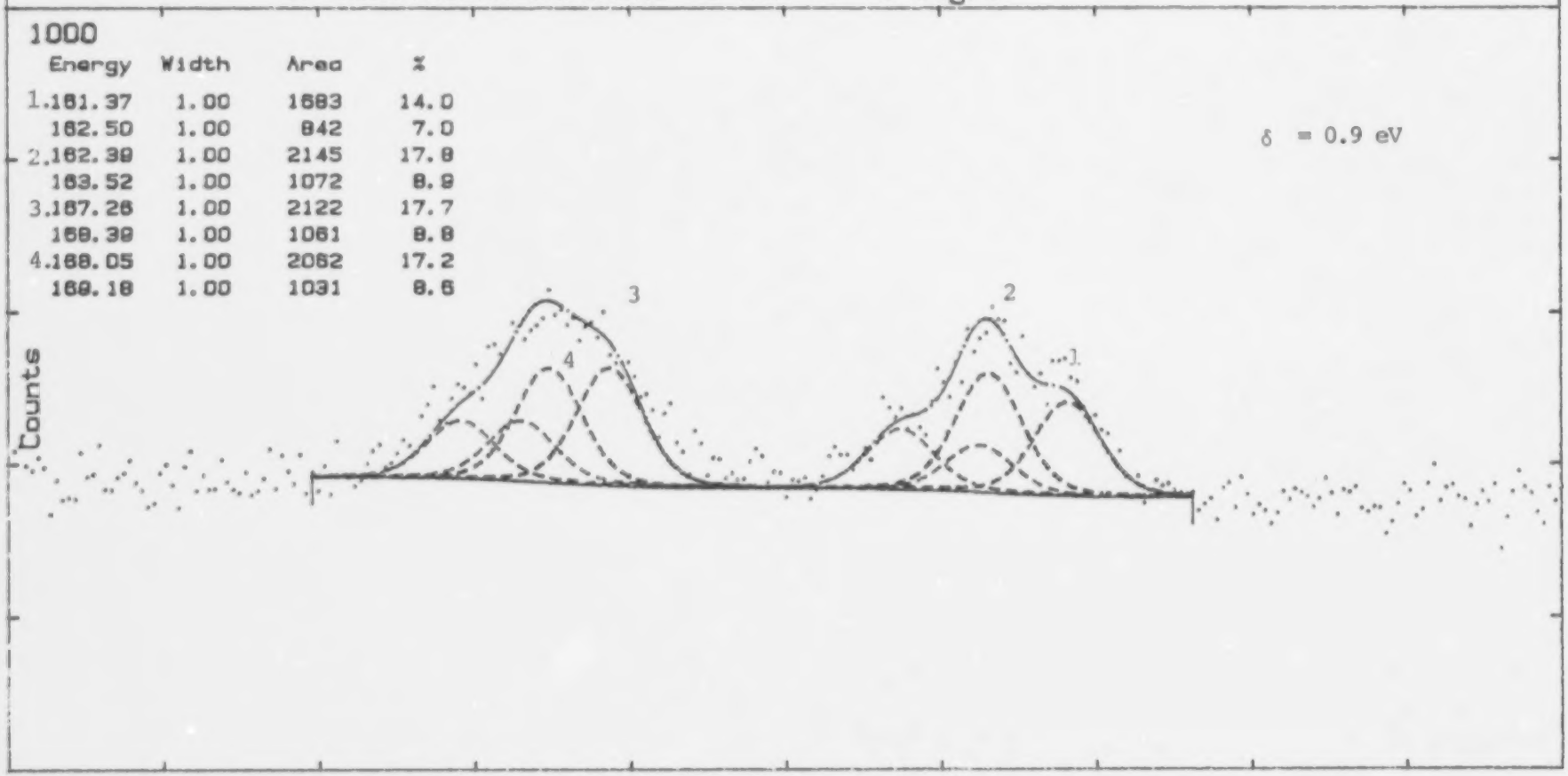

175.0 Binding Energy (eV) 155.0

SURFACE SCIENCE WESTERN University of Western Ontario

File: RRM3_16A	Date: 6/24/1986	Spot Size: 300 u	Flood Gun: 1.0 eV
Region 4	Disc: RRM02	# of Scans: 10	Resolution: 2
Description: FUSINITE RRM3_16 AFTER 15 HRS. EXPOSURE TO AIR AT 70 degrees C			Operator: JRM

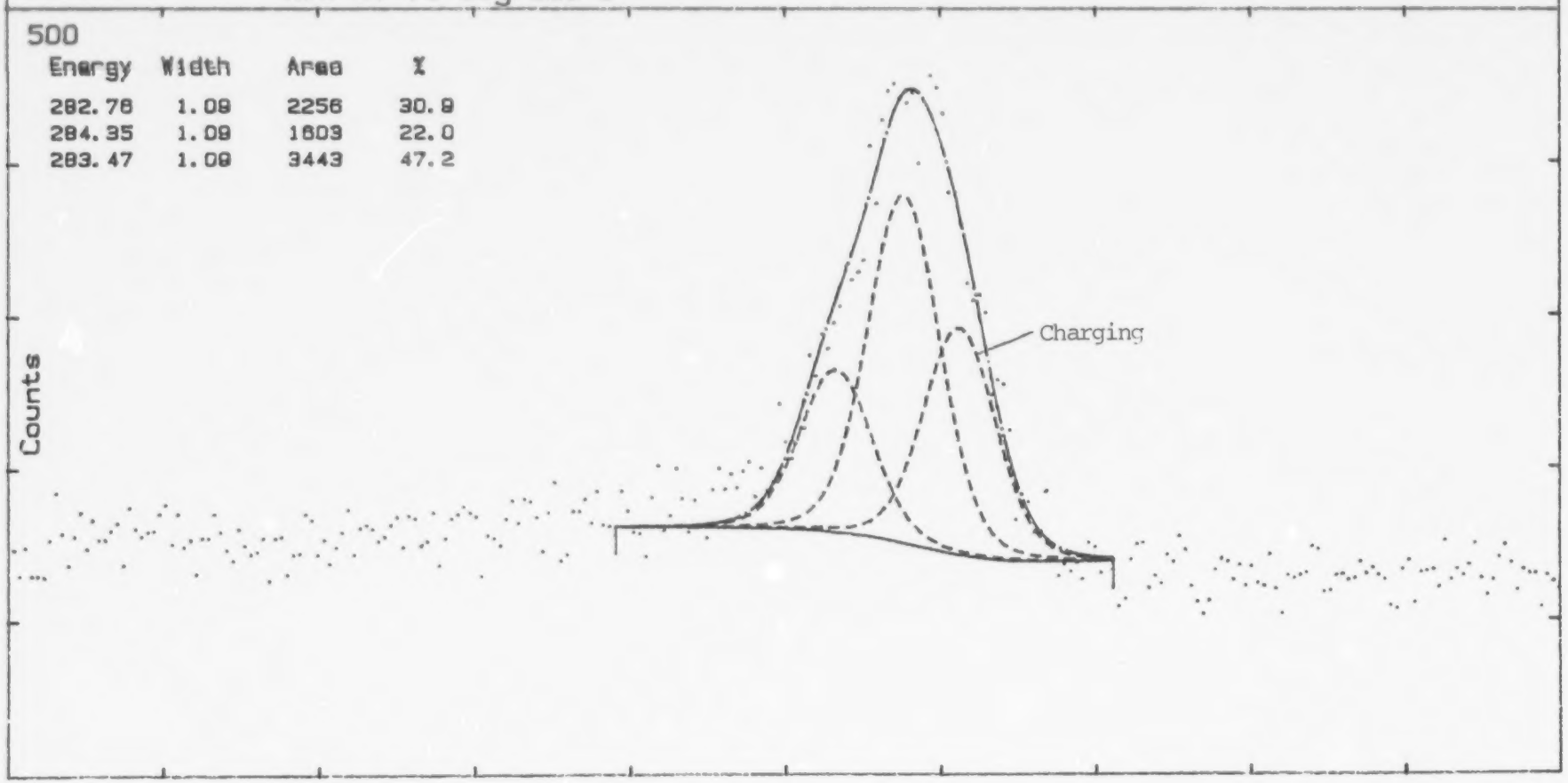

SURFACE SCIENCE WESTERN University of Western Ontario

File: RRM3_15	Date: 6/20/1986	Spot Size: 1000 u	Flood Gun: 1.0 eV
Region 2	Disc: RRM02	# of Scans: 2	Resolution: 4
Description: FUSINITE CLEAVED UNDER N2 (4:40PM), SPETRA STARTED APPROX. 35 MIN. LATTER.			Operator: JRM

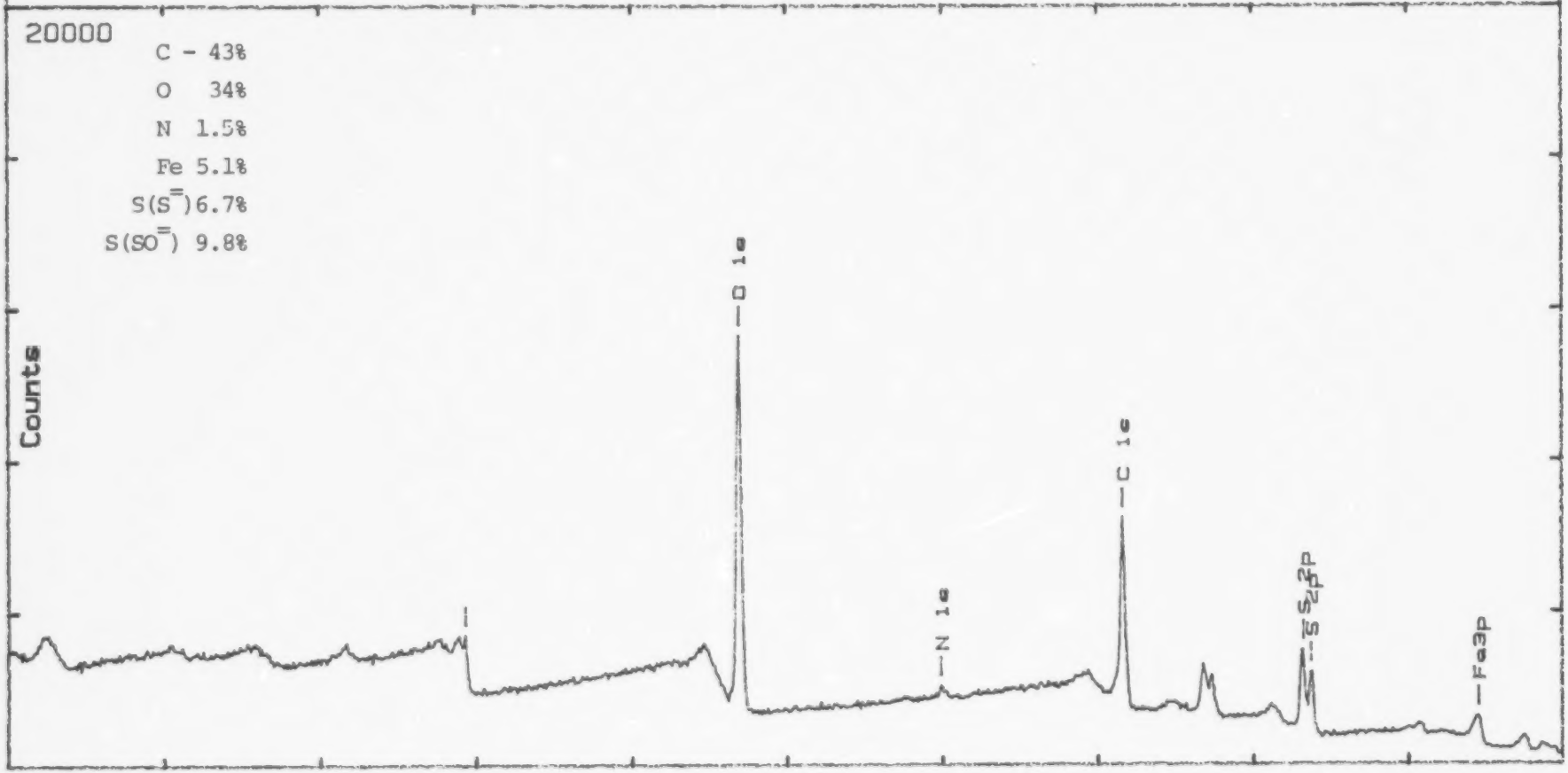

SURFACE SCIENCE WESTERN University of Western Ontario

Report #: CANMET

File: RRM3_15	Date: 6/20/1986	Spot Size: 300 u	Flood Gun: 1.0 eV
Region 1	Disc: RRM02	# of Scans: 20	Resolution: 2

Description: FUSINITE CLEAVED UNDER N2 (4:40PM), SPETRA STARTED APPROX. 35 MIN. LATTER.

Operator: JRM

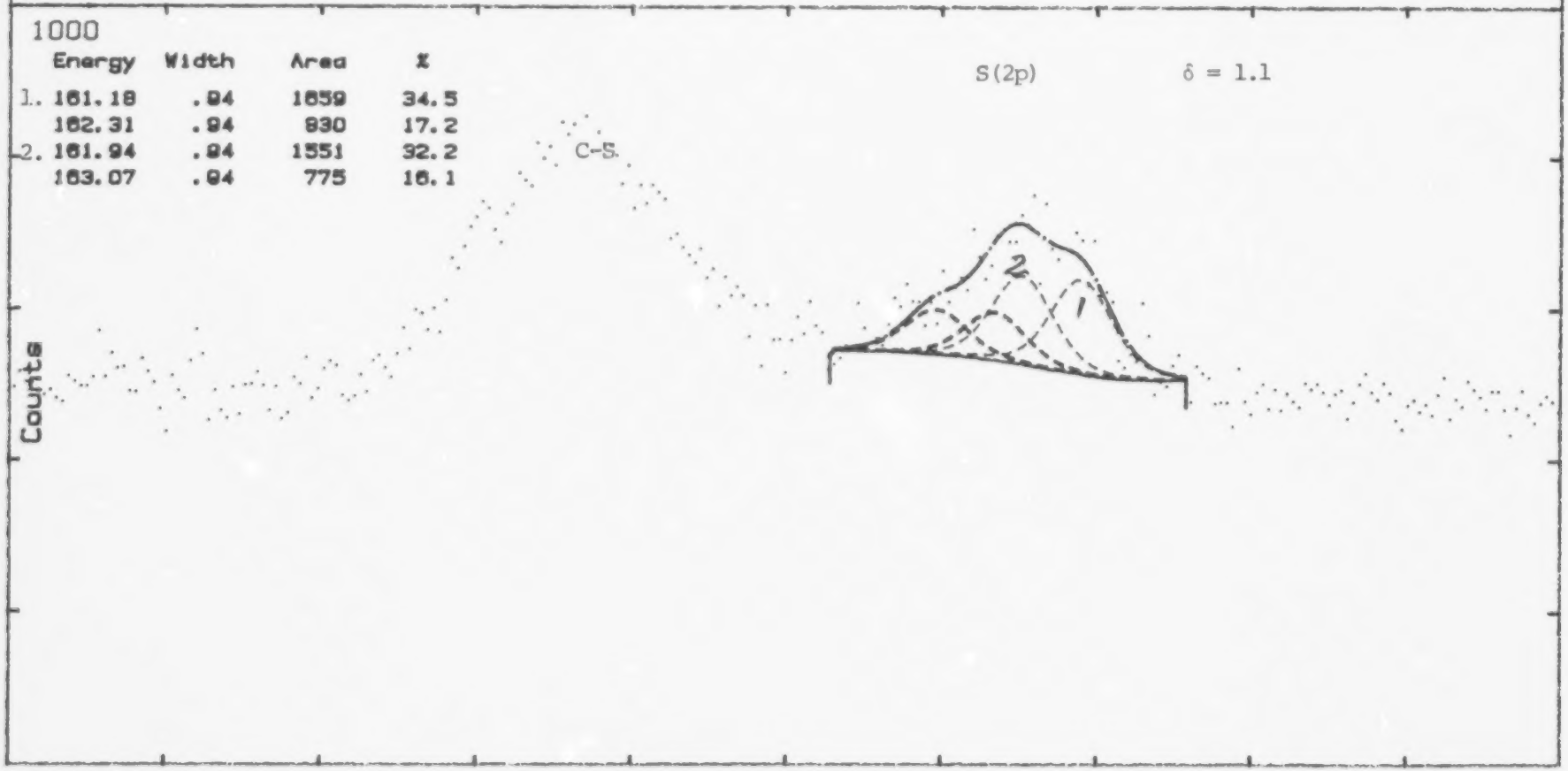

175.0 **Binding Energy (eV)** 155.0

SURFACE SCIENCE WESTERN University of Western Ontario

Report #: CANMET

File: RRM3_15	Date: 6/20/1986	Spot Size: 300 u	Flood Gun: 1.0 eV
Region 1	Disc: RRM02	# of Scans: 20	Resolution: 2
Description: FUSINITE CLEAVED UNDER N2 (4:40PM). SPETRA STARTED APPROX. 35 MIN. LATTER.			Operator: JRM

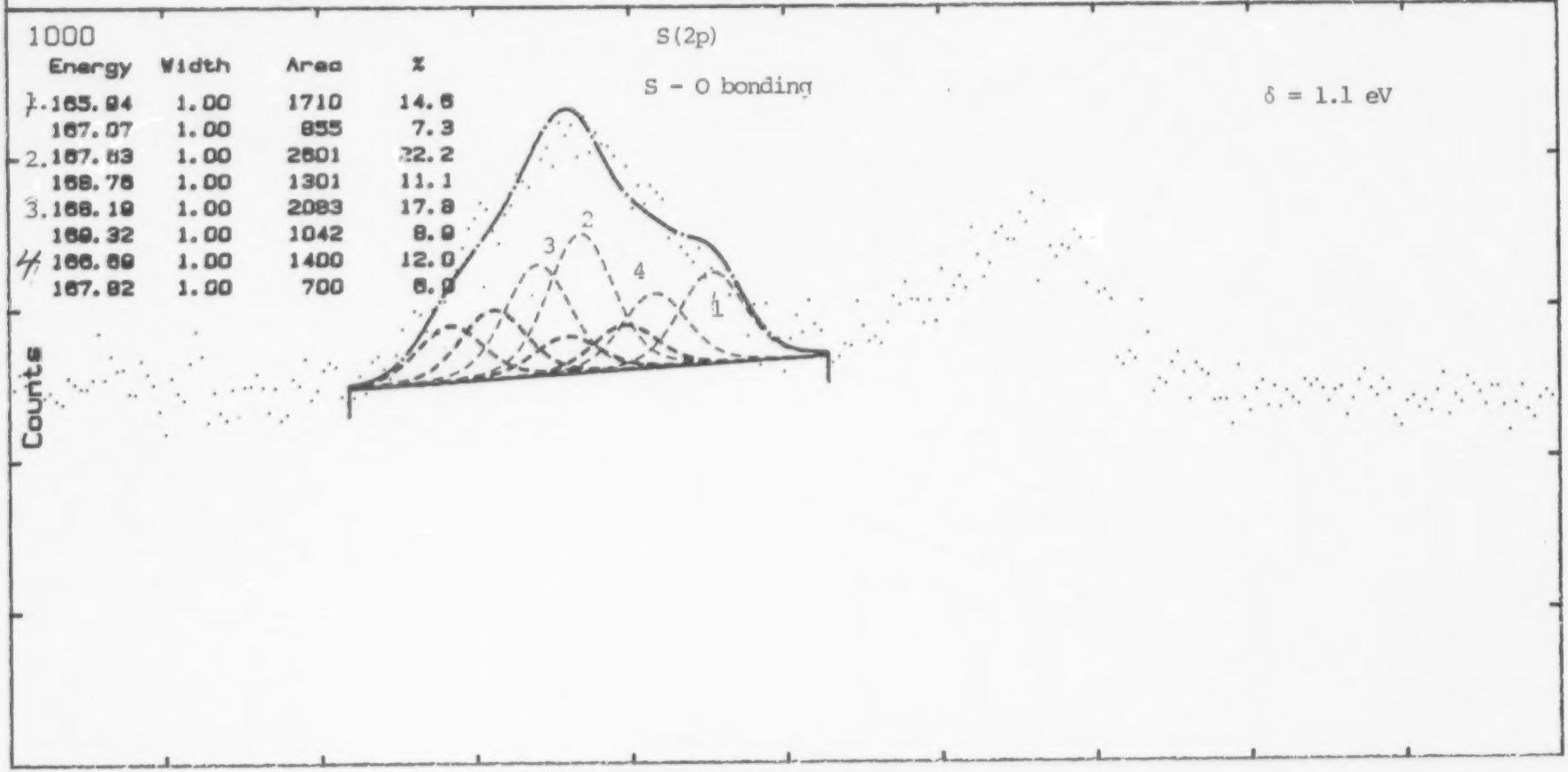

175.0 **Binding Energy (eV)** 155.0

SURFACE SCIENCE WESTERN University of Western Ontario **Report #:** CANMET

File: RRM3_15A	Date: 6/23/1986	Spot Size: 1000 u	Flood Gun: 1.0 eV
Region 1	Disc: RRM02	# of Scans: 2	Resolution: 4

Description: FUSINITE CLEAVED UNDER N2 (4:40). SPECTRA TAKEN AND ALLOWED 60 HRS. AIR EXPOSURE, SPECTRA RETAKEN **Operator:** JRM

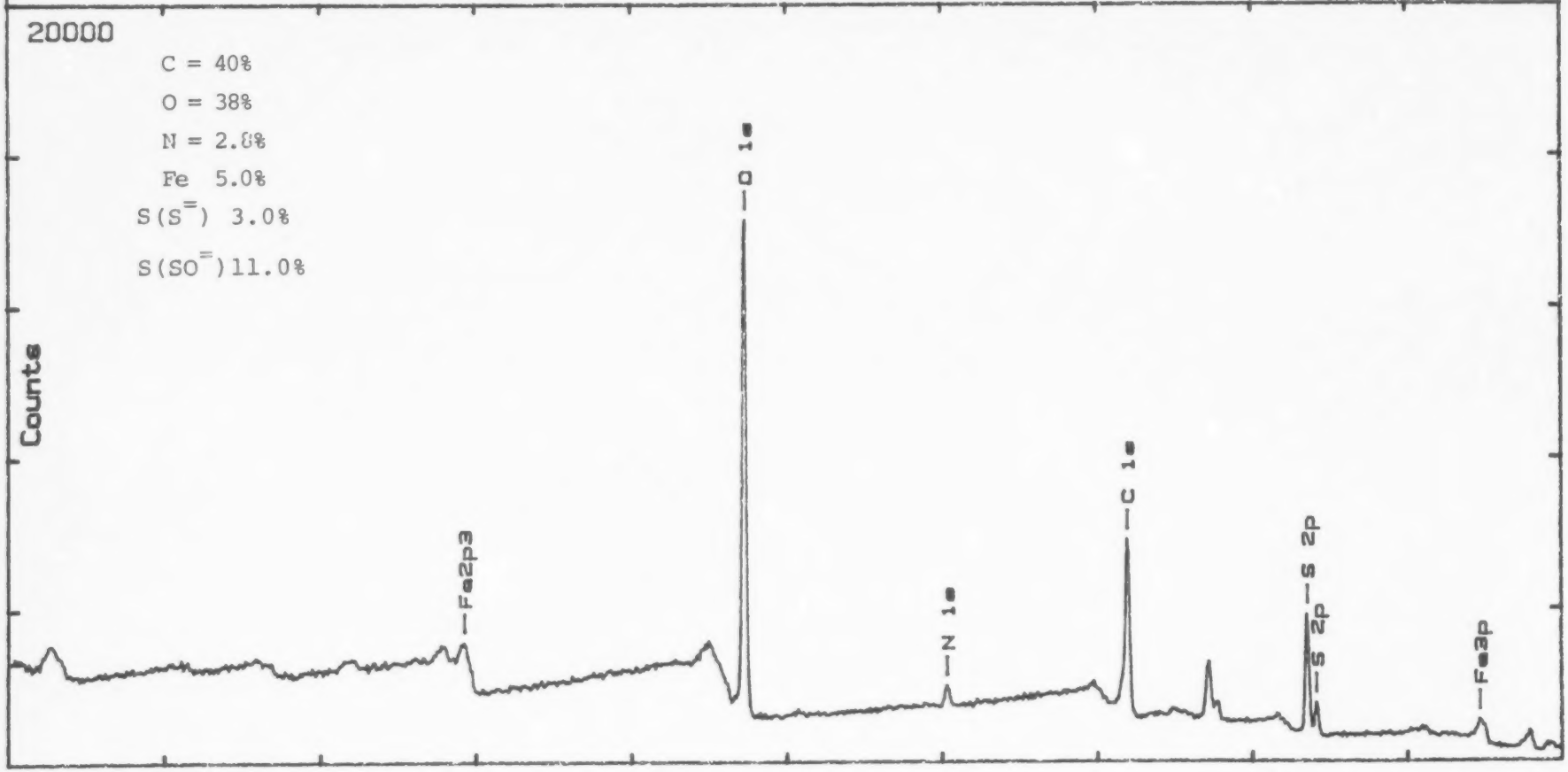

SURFACE SCIENCE WESTERN University of Western Ontario **Report #:** CANMET

File: RRM3_15A	Date: 6/23/1986	Spot Size: 300 u	Flood Gun: 1.0 eV
Region 2	Disc: RRM02	# of Scans: 20	Resolution: 2

Description: FUSINITE CLEAVED UNDER N2 (4:40). SPECTRA TAKEN AND ALLOWED 60 HRS. AIR EXPOSURE, SPECTRA RETAKEN **Operator:** JRM

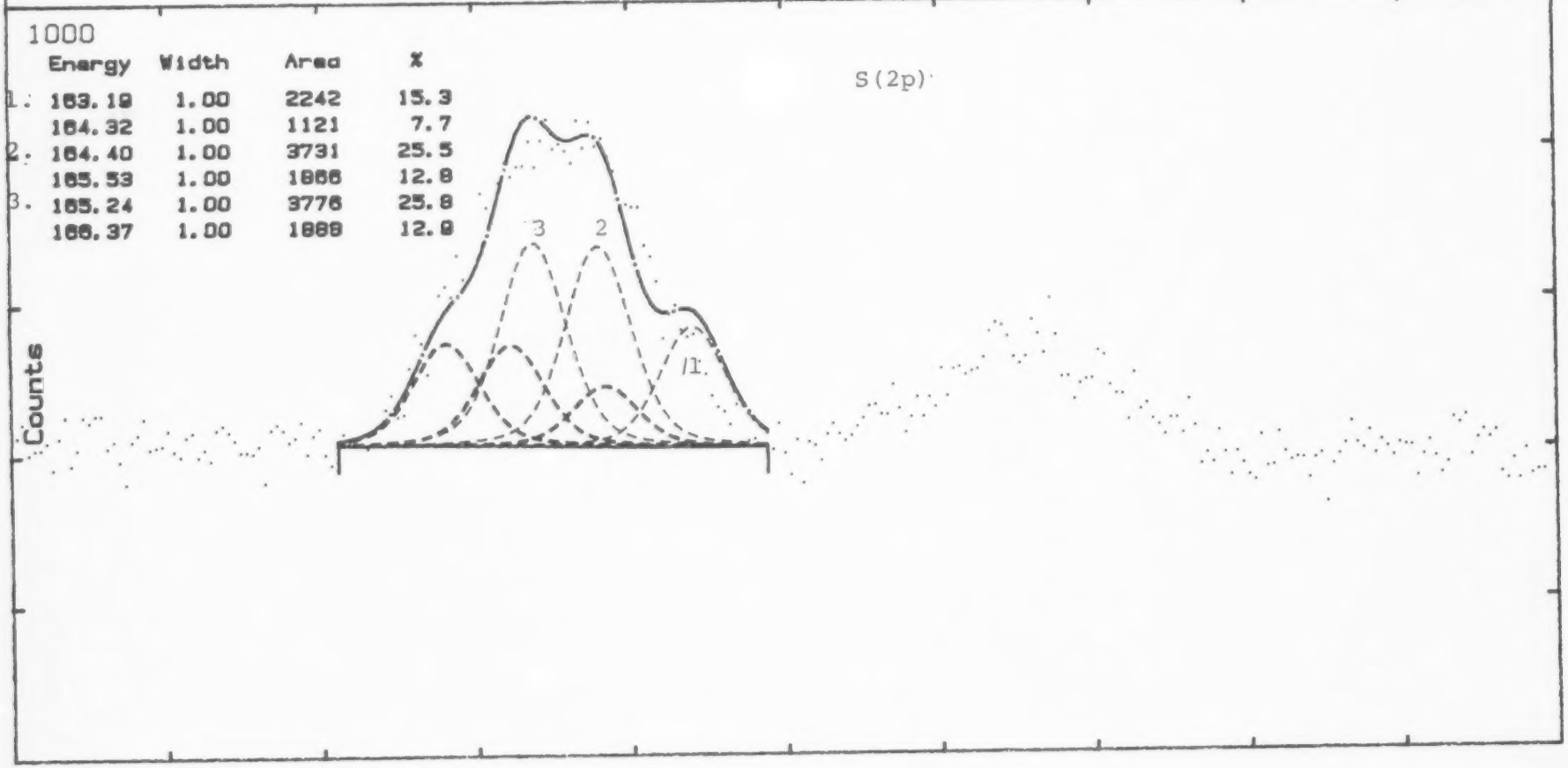

SURFACE SCIENCE WESTERN University of Western Ontario

Report #: CANMET

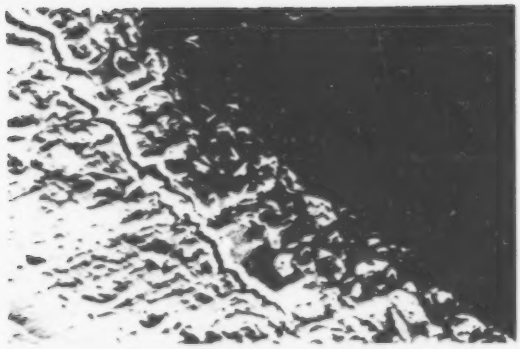

A. SEM Photograph

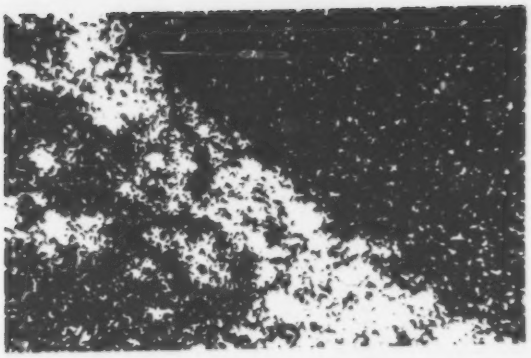

B. EDX of Si distribution

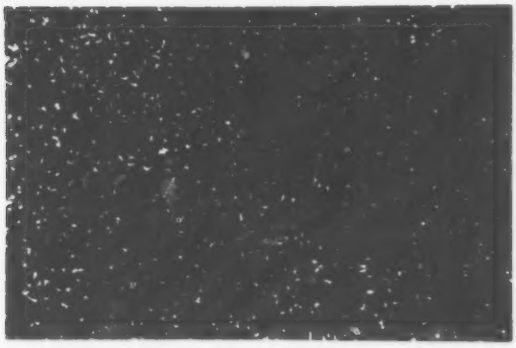

C. EDX of K distribution

D. SIMS step scan across boudary for Al and K

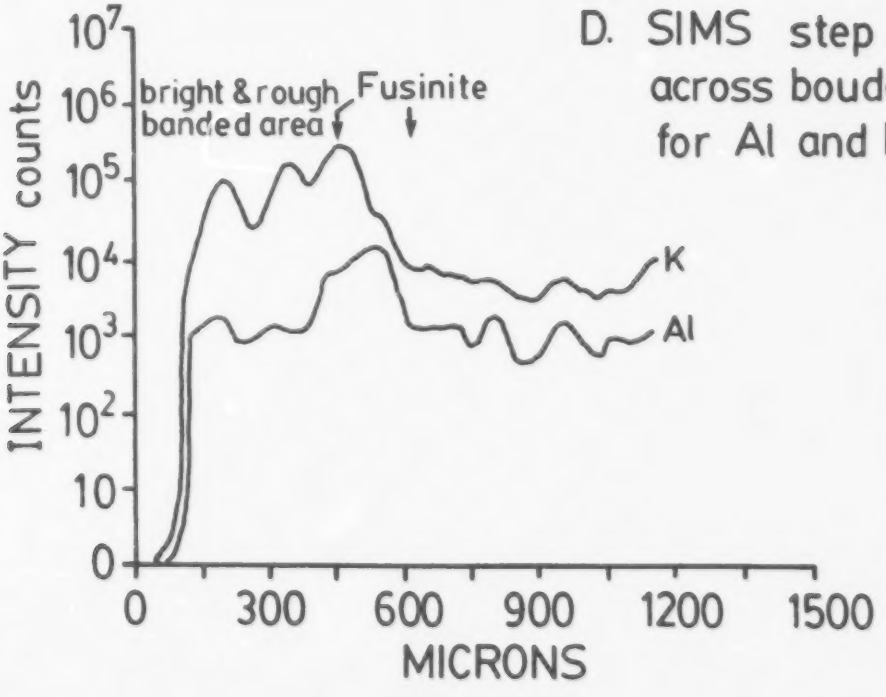

Fig. 18

C_2^- 1/4 s

Si^+ 30 s

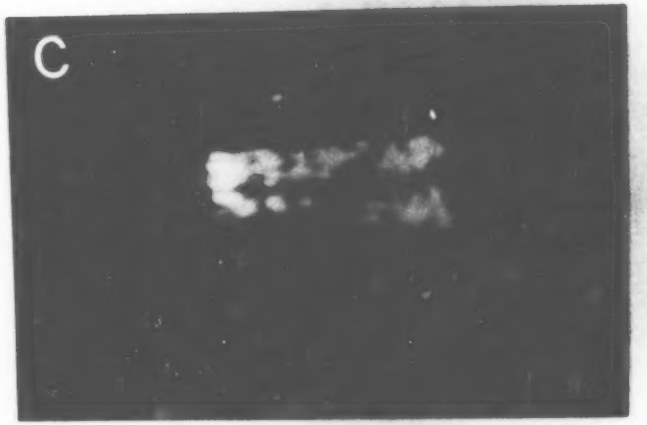

Al^+ 10s

K^+ 60s

Fig. 19

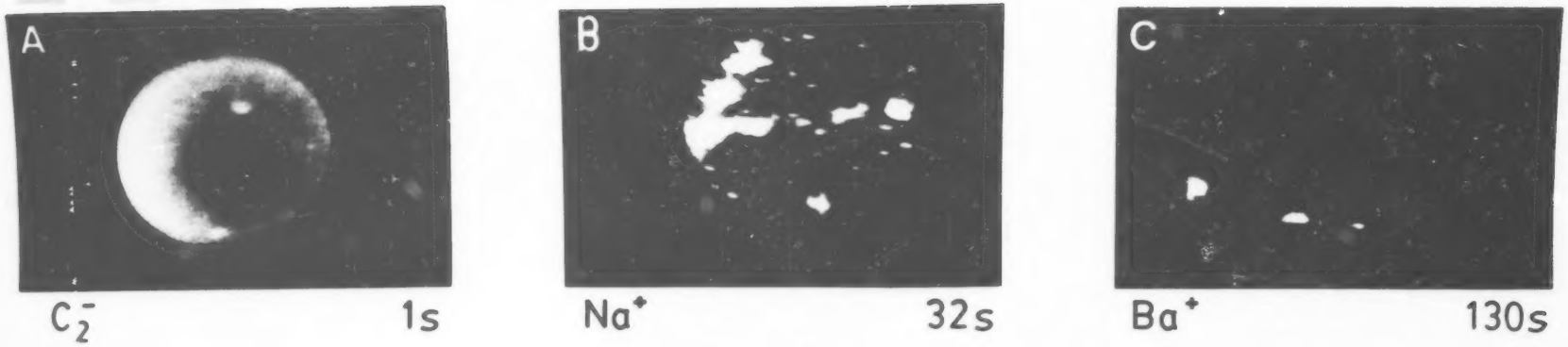

Fig. 20

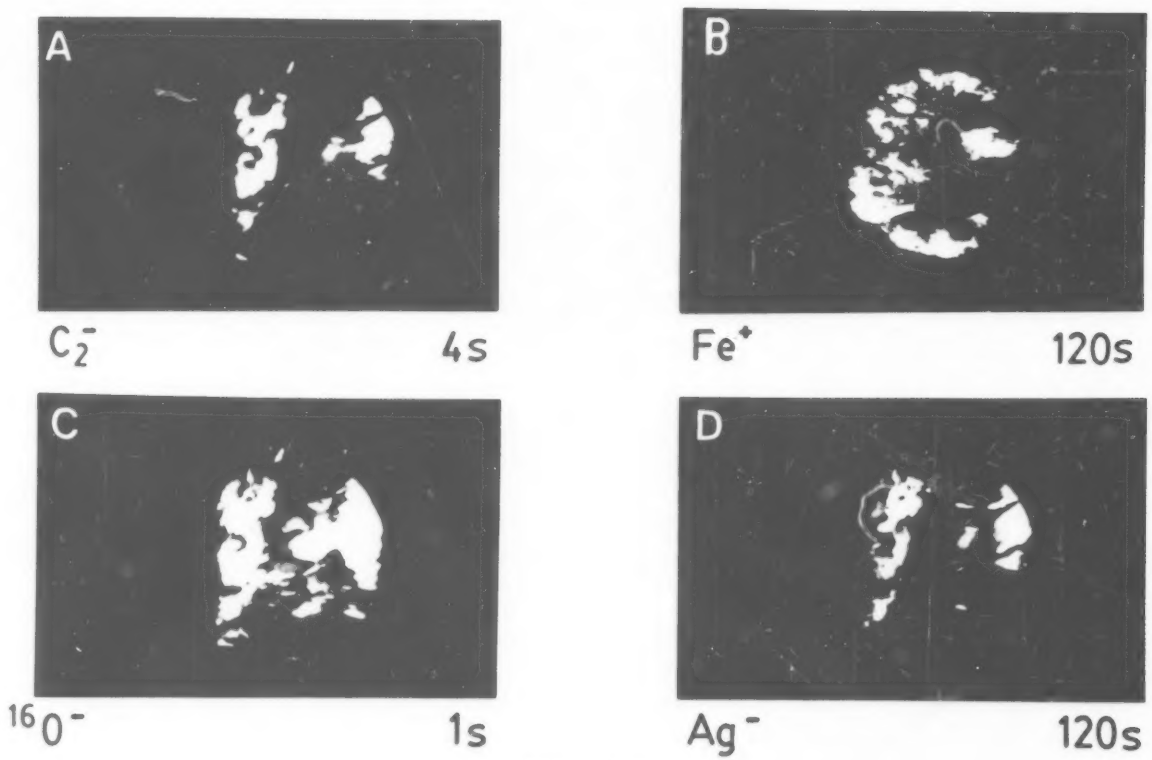

Fig. 21

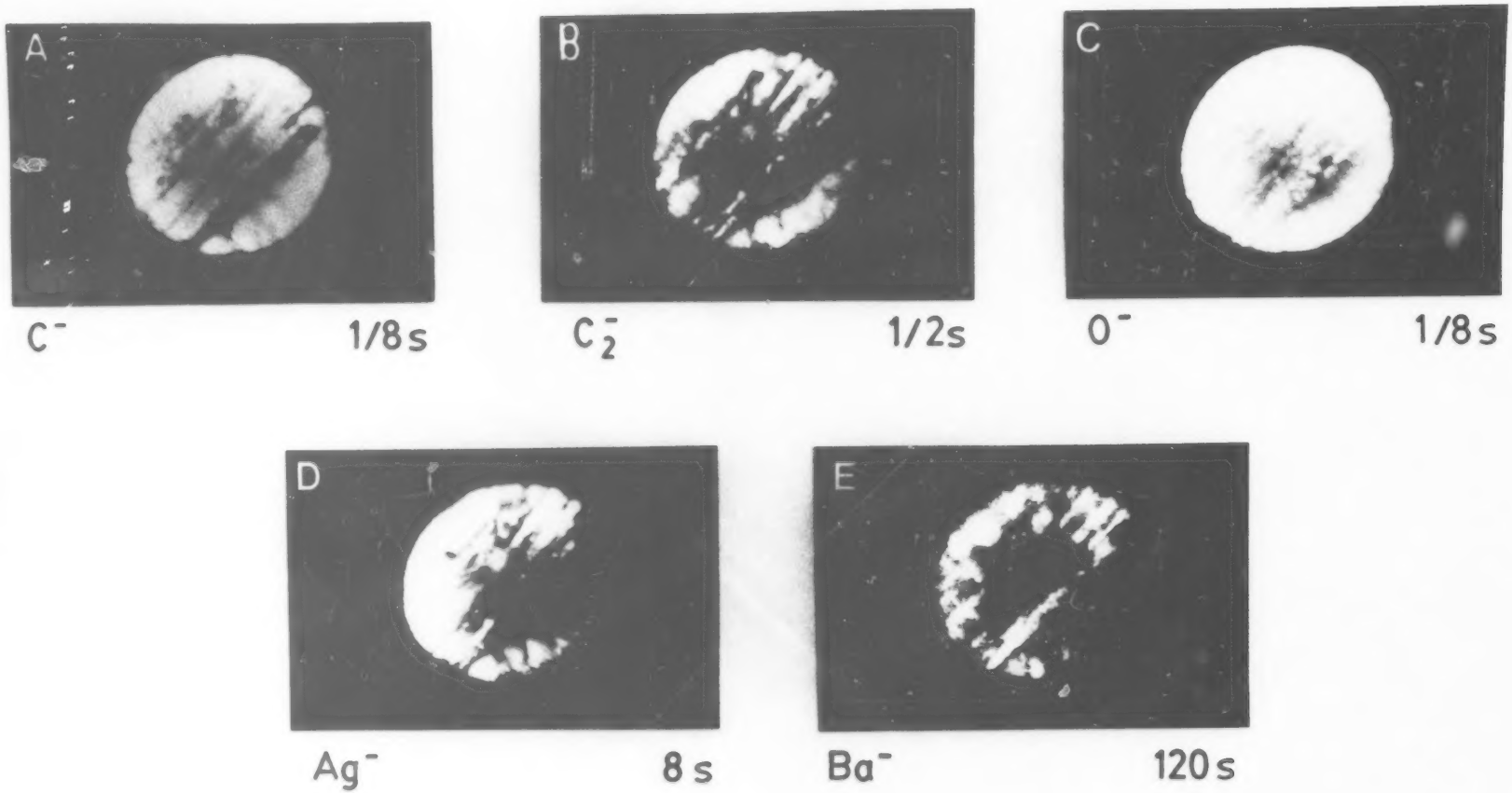

Fig. 22

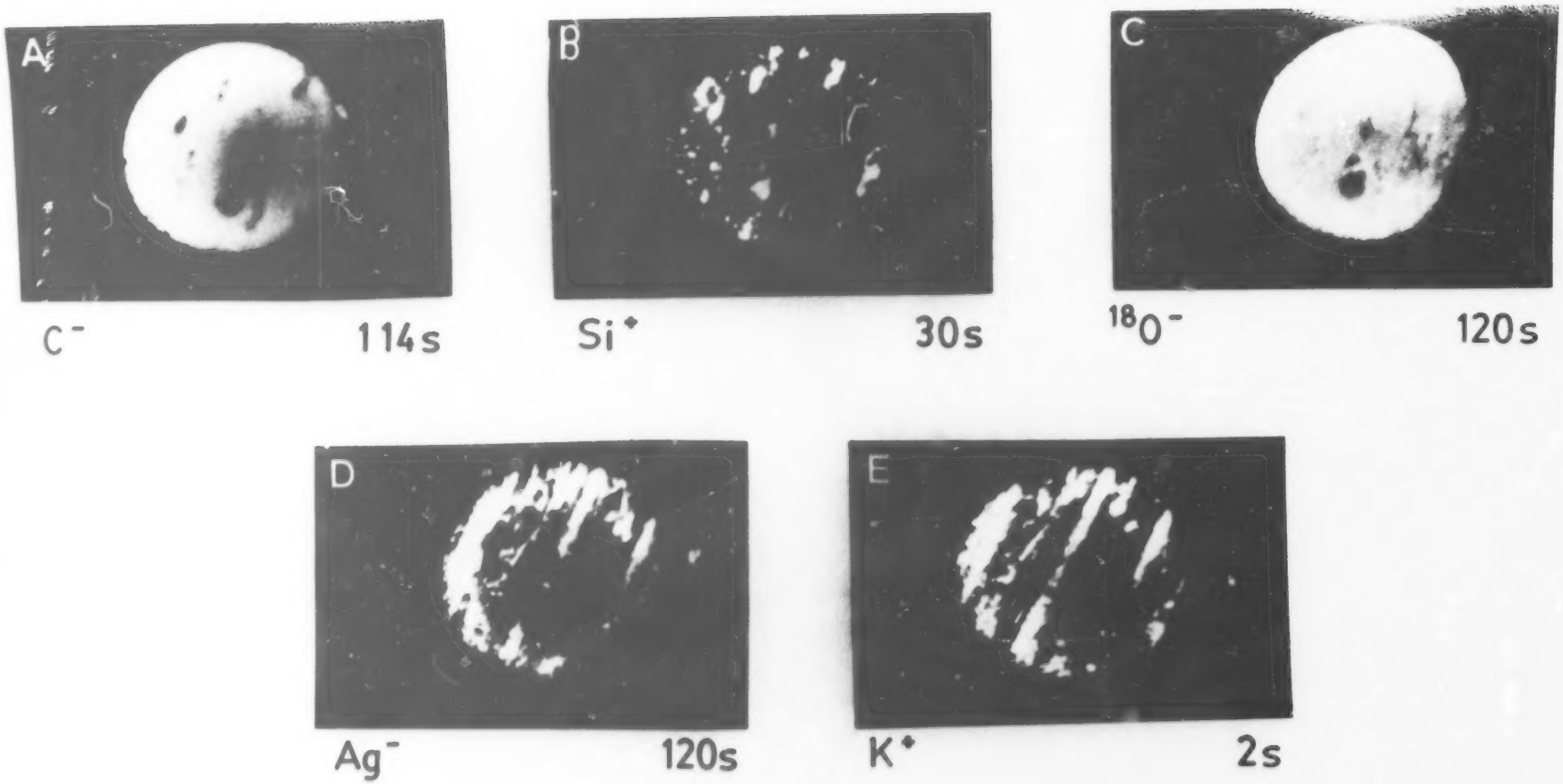

Fig. 23